JOURNAL OF GEOPHYSICAL RESEARCH, VOL. 101, NO. C2, PAGES 3675–3696, FEBRUARY 15, 1996

Southern Ocean fronts from the Greenwich meridian to Tasmania

Igor M. Belkin[1]

Shirshov Institute of Oceanology, Russian Academy of Sciences, Moscow, Russia

Arnold L. Gordon

Lamont-Doherty Earth Observatory, Columbia University, Palisades, New York

Abstract. All available meridional sections have been analyzed to investigate the evolution of main fronts between 0° and 150°E. The central South Atlantic is featured by the Subtropical Frontal Zone (STFZ), bordered by the North and South Subtropical Fronts (NSTF and SSTF, respectively), and by the Polar Frontal Zone (PFZ), bordered by the Subantarctic and Polar Fronts (SAF and PF, respectively). This structure becomes more complex in the African sector as the Agulhas Retroflection and the bottom topography force a more convoluted pattern. The Retroflection and associated Agulhas Front (AF) press the SSTF from 38° to 42°-43°S. Strong interactions of the AF, SSTF, and SAF with topography shift the fronts but do not obliterate them. The AF can be traced reliably up to 52°E, sometimes up to 75°E. The SAF is deflected from 45° to 43°S by the Mid-Ocean Ridge and converges with the SSTF north of the Prince Edward Islands to form a combined SSTF/SAF. This front intensifies east of 50°-52°E as a result of the confluence with the AF, and between 52° and 65°E a triple AF/SSTF/SAF ("the Crozet Front") is observed. The PF continues along 49° and 50°S between the Crozet Plateau and the Ob-Lena (Conrad) Rise, passing north of Kerguelen, nearly joining the triple Crozet Front. Downstream of the Kerguelen-Amsterdam Passage the canonical structure is being restored (SSTF, SAF, PF); however, the front parameters in the Australian sector are different from the African sector, largely because of strong air-sea interaction and cross-frontal exchanges in the Crozet-Kerguelen region. The SSTF, squeezed between the AF and SAF, loses characteristics to both. The SSTF/SAF interaction results in the Australian SAF being warmer and saltier downstream, while the SSTF becomes shallower and weaker. The Australian STF derives its characteristics mostly from the AF, thus bringing the modified Agulhas waters to the Pacific Ocean. The newly defined North Subtropical Front (NSTF) was distinguished in the Indian Ocean between 31° and 38°S. The front marks the southern boundary of the subtropical salty, warm water pool of the central South Indian Ocean. The NSTF location is coincident with the position of the wind convergence between westerlies and easterlies, suggesting the possible wind-driven frontogenesis.

1. Introduction

The main feature of the Southern Ocean is its conspicuous frontal banding consisting of several circumpolar quasi-uniform belts divided by fronts, comparatively narrow zones of sharp changes in vertical structure, temperature, salinity, and nutrients. The early investigators recognized existence of two principal fronts, the Subtropical Convergence (STC) or Subtropical Front (STF), which separates subtropical and subantarctic waters, and the Antarctic Convergence (AC) or Polar Front (PF), dividing subantarctic and Antarctic waters [*Meinardus*, 1923; *Böhnecke*, 1936; *Deacon*, 1933, 1937; *Sverdrup et al.*, 1942; *Mackintosh*, 1946; *Houtman*, 1964; *Gordon*, 1967; *Gordon and Goldberg*, 1970].

In the 1960s, a detailed study of the PF based on R/V *Eltanin* data gave birth to the concept of the Antarctic Polar Front Zone [*Gordon*, 1967, 1971; *Gordon et al.*, 1977a], transformed later into the concept of the Polar Frontal Zone (PFZ) bordered by two fronts, the Subantarctic Front (SAF) on the north, and the Polar Front on the south [*Emery*, 1977; *Sievers and Emery*, 1978; *Patterson and Sievers*, 1979/1980; *Nowlin et al.*, 1977; *Joyce et al.*, 1978; *Whitworth*, 1980; *Nowlin and Clifford*, 1982; *Clifford*, 1983; *Sievers and Nowlin*, 1984; *Scientific Committee on Oceanic Research*, 1985; *Nowlin and Klinck*, 1986; *Belkin et al.*, 1991; *Belkin*, 1993b]. South of the PF is the Antarctic Zone. In the South Atlantic, inside the Antarctic Zone, another frontal zone has been distinguished, the Weddell-Scotia Confluence (WSC) [*Gordon*, 1967; *Patterson and Sievers*, 1980]. The STF, the SAF, and the PF are associated with the filaments of

[1]Also at Ocean Climate Laboratory, National Oceanographic Data Center, NOAA, Washington, D.C.

Paper number 95JC02750.
0148-0227/96/95JC-02750$05.00

the Antarctic Circumpolar Current (ACC)[*Nowlin et al.*, 1977; *Joyce et al.*, 1978]. Analysis of the First GARP Global Experiment (FGGE) 1978-1979 drifter data set revealed the convergent nature of these fronts [*Hofmann*, 1985].

In the South Atlantic and the South Pacific the STF has been found to have a double structure, consisting of the North and South STF [*Belkin*, 1988a, 1993a, 1994].

Fronts of the southern Indian Ocean were studied fragmentarily, mainly south of Africa, where an additional feature, the Agulhas Front (AF), was identified [*Lutjeharms*, 1985; *Lutjeharms and Valentine*, 1984], or south of Australia [*Burling*, 1961; *Edwards and Emery*, 1982]. The central part of this ocean only recently became the subject of frontal research [*Gambéroni et al.*, 1982; *Belkin*, 1988b, 1989a,b, 1990; *Nagata et al.*, 1988; *Park et al.*, 1989, 1991, 1993; *Stramma*, 1992].

The southeast Atlantic and Indian Ocean sectors (Figure 1) are featured by a complicated frontal structure, with striking regional differences. In this work we have investigated all the aforementioned main open ocean fronts, from the Greenwich meridian to Tasmania, in the region 30°-60°S, 0°-150°E, focusing mostly on the spatial variability of the fronts. The zonal variability of the fronts was studied as well but will be reported in detail elsewhere.

2. Data

The main subject of this study is the meridional structure of quasi-zonal fronts, therefore we used primarily quasi-meridional sections (~200 sections). Principal data sources are categorized as follows:

(1) high-quality deep conductivity-temperature-depth (CTD) sections of *Discovery* cruises 164 and 165A; *Eltanin* cruises 34 to 37, 39, 41, 44, 45, 49, 50, and 54; *Islas Orcadas* Cr. 11 and 12; *Knorr*/Ajax; *Knorr* cruise 104-5/ARC; *Marion Dufresne* cruises 12, 38, 43, 48, 53, and 68; *Meteor* cruise 11/SAVE-7; *Robert D. Conrad* cruise 17; and *S.A.Agulhas*/SCARC; (2) CTD/bottle data obtained by research vessels of the Shirshov Institute of Oceanology, Russian Academy of Sciences (IORAS), Moscow (*Akademik Mstislav Keldysh* cruise 5; *Dmitry Mendeleev* cruises 11 and 16; *Vityaz I* cruise 33; and *Vityaz II* cruises 4 and 13; (3) CTD/bottle data obtained by vessels of the Russian Hydrometeorological Service's institutions, Arctic and Antarctic Research Institute (AARI, St.Petersburg) (*Ob* cruises 1, 2, and 6 to 15; *Mikhail Somov* cruise 7; *Professor Vize* cruises 7, 10, 13, 19, 22, 24, 32, 34, 36, and 43; *Professor Zubov* cruises 1, 6, 11, 20, and 24; Far-East Research Institute (Russian abbreviation DVNII, Vladivostok) (*A.I.Voeikov* cruises 17, 19, 20, 22, and 23; *Akademik Korolev* cruises 9, 15, 17, and 29; *Akademik Shirshov* cruises 5, 9, and 14; *Yu.M.Shokalsky* cruises 20, 32, 33, and 38); (4) CTD/bottle data obtained during fishery/biological surveys by former Soviet Union (FSU) ships belonging to the YugNIRO (Southern Institute of Fisheries and Oceanographic Research, Kerch, Crimea, Ukraine) (*Aelita* cruises 1, 2, and 19; *Ariel* cruise 9, *Chatyr-Dag* cruises 2, 15, and 16; *Chernomor* cruise 9; *Fiolent* cruises 1, 2, 12, 16, 21, 22, and 26; *Geroevka* cruise 6; *Kalper* cruise 13; *Kara-Dag* cruises 2 to 5, 11, and 16; *Marlin* cruises 9 to 13; *Mys Ostrovskogo* cruise 14; *Myslitel* cruise 13; *Novoukrainka* cruise 7; *Professor Mesyatsev* cruises 7, 17 to 20, and 22; *Skif* cruises 2, 3, 5, 6, 9, 10, 14, 18, and 24; *Zvezda Azova*

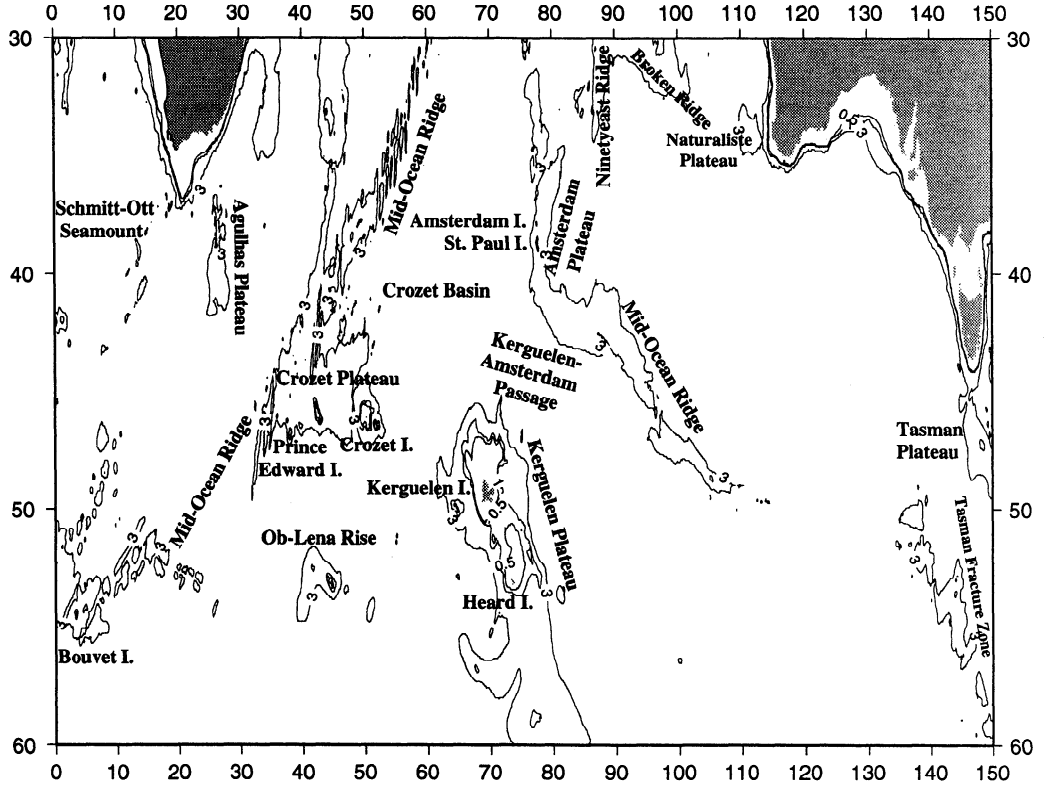

Figure 1. Bottom relief and place names of the study area. The isobaths shown are 0.5, 1, and 3 km.

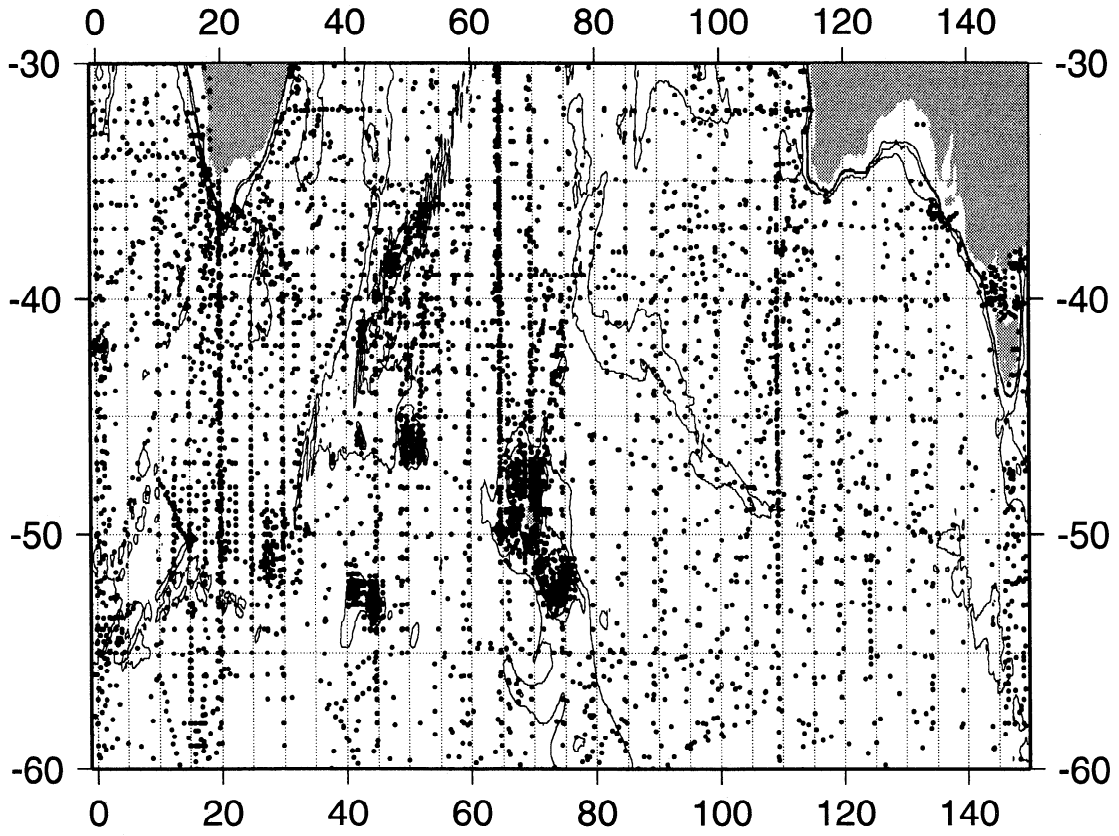

Figure 2. Oceanographic stations used in the analysis (>25,000 stations).

cruises 7 and 10; *Zvezda Chernomoria* cruises 5 and 7; and *Zvezda Sevastopolya* cruise 3; (5) CTD/expendable bathythermograph (XBT)/bottle data obtained by Japanese vessels *Umitaka Maru III* (Tokyo University of Fisheries), *Hakuho Maru* (Ocean Research Institute, University of Tokyo), and *Kaiyo Maru* (National Research Institute of Far Seas Fisheries, Japan Fisheries Agency) during the Biological Investigations of Marine Antarctic Systems and Stocks (BIOMASS) [*Hoshiai et al.*, 1991]; (6) XBT/station data obtained during relief voyages of supply vessels of Antarctic expeditions: *Soya*, *Fuji*, and *Shirase* (Japanese Antarctic Research Expedition, JARE), *Gallieni* and *Marion Dufresne* (Terres Australes et Antarctiques Francaises), *S.A.Agulhas* (South African National Antarctic Expedition); and (7) bottle data of *Diamantina* (Commonwealth Scientific and Industrial Research Organisation, Australia) across the Subtropical Front.

The FSU data were obtained from the World Data Center-B (Obninsk, Russia), and from YugNIRO. The data set of *Gordon et al.* [1982] was used as well. Other data were obtained as data reports and digitized at the Lamont-Doherty Earth Observatory (LDEO, Palisades, New York) and IORAS. All the data (>25,000 stations) are now stored in the LDEO computerized data base (Figure 2).

Our data quality control follows general concepts of *Levitus* [1982], *Gordon et al.* [1982] and *Belkin* [1984a,b, 1991], elaborated by *Olbers et al.*[1992]. The contoured vertical temperature-salinity (T-S) sections were especially useful for elimination of gross errors. The T-S scatter diagrams for individual cruises were instrumental for detection of outliers and dubious cruises with high T-S dispersion. *Akademik Vernadsky* cruise 24 and *Vityaz II* cruise 13 were discarded because of anomalously high salinity values. Some cruises were partially discarded, for example, *Professor Zubov* cruise 24 and *Professor Vize* cruise 32 (comprising the POLEX-South-78 survey), whose salinities are mutually inconsistent. The latter two cruises were discarded also by *Olbers et al.*[1992].

The data set of *Gordon et al.*[1982] was edited earlier; its superior quality was asserted by *Olbers et al.*[1992]. The YugNIRO data apparently were not edited before. We screened this data set to eliminate gross errors identified on contoured sections. We left intact some lens-like objects with significant T and S anomalies, if these anomalies were density-compensating [*Kostianoy and Belkin*, 1989].

3. Definition and Determination of Fronts

3.1. Method

Fronts are identified by marked changes in vertical structures from one side to the other. Such changes are usually accompanied by enhanced horizontal property gradients at various levels and concentrated geostrophic flow. In the present paper, temperature and salinity are the properties utilized. The particular values of the properties within fronts can change both temporally and downstream as a result of gradual modification of the adjacent water masses by nonfrontal processes (such as air-sea interaction) and cross-frontal mixing.

To trace the varying fronts reliably, one needs: (1) a dense database of meridional sections spaced ~2°-3° in longitude (at this distance, air-sea interaction and cross-frontal mixing would not produce significant changes of frontal *T-S* characteristics); (2) a set of several levels to be used simultaneously for frontal tracing because there is no single depth equally suitable for tracing all the fronts and because this is necessary to eliminate influence of intrusions and lenses of limited vertical extent that are widespread near fronts [*Kostianoy and Belkin*, 1989]; and (3) an ensemble of adjustable numerical criteria that should be modified in the along-front direction following the observed gradual evolution of frontal *T-S* ranges, so the study of zonal variability of fronts should proceed concurrently with frontal tracing.

Table 1. Criteria for PF Identification

Criterion	References
Location where the T_{min} dips below 200 m	*Deacon* [1933], *Mackintosh* [1946], *Ostapoff* [1962], *Gordon* [1967], *Lutjeharms and Emery* [1983], *Peterson and Whitworth* [1989]
Northern limit of the subsurface temperature inversion	*Garner* [1958]
Northern extent of the 1°C isotherm in the T_{min} layer	*Burling* [1961]
Axis of the S_{min} belt at the 200 m surface	*Ostapoff* [1962], *Gordon et al.* (1978), *Taylor et al.* [1978]
Northern terminus of the subsurface T_{min} layer bounded by the 2°C isotherm in the 100-300 m layer (summer); vertical 2°C isotherm (winter)	*Botnikov* [1963], *Joyce et al.* [1978], *Lutjeharms* [1985] (without a specified layer), *Lutjeharms and Emery* [1983], *Lutjeharms and Valentine* [1984] (at 200 m), *Park et al.* [1993]
Position where the T_{min} layer ends or its depth changes abruptly	*Gordon* [1967]
grad T_0 > 2°C/0.5°latitude	*Gordon* [1967]
Position where the T_{min} layer begins its rapid descent	*Gordon* [1971]
Northern extent of the 0°C isotherm associated with the T_{min} layer	*Nowlin et al.* [1977], *Nagata et al.* [1988]
Northern edge: T_{200} = 2°C	*Clifford* [1983]
Sinking of the T_{min} from 100 m to >=300-400 m	*Whitworth and Nowlin* [1987]
Axial T_{100}=3°C	*Nagata et al.* [1988]
Diving of the T_{min} through the 200 to 400 m layer	*Patterson and Whitworth* [1990]
Axial T_{200}=2°C	*Orsi et al.* [1993]
T<2°C along the T_{min} at Z<200 m, farther south; T_{min} (if present) at Z>200 m, farther north; T>2.2°C along T_{max} at Z>800 m, farther north	*Orsi et al.* [1995]

With all this in mind we have assembled all available meridional sections into a dense array of some 200 sections between 0° and 150°E, most of them crossing several fronts. This database allowed us to trace fronts consistently, following their gradual spatial evolution.

To this end, for each frontal crossing we determined up to 23 parameters including T and S at 0, 200, 400, and 600 m north and south of a front, and the 10°C depth and salinity for the Agulhas Front and the Subtropical Front, and the T_{min} depth and salinity for the Polar Front. The "parameter-longitude" plots were constructed for all the parameters. The *T-S* diagrams for each front and level, the warm/cold sides separately, were constructed as well and used in the analysis.

We expect a particular front to belong to prescribed *T-S* ranges (at each specified depth), and at the same time we expect the ranges to be changed gradually downstream reflecting evolution of the front.

While the study is dedicated mainly to the southern Indian Ocean fronts, we started from the Greenwich meridian because the frontal structure "upstream" of the Agulhas Front is simpler. The bulk of high-quality CTD sections is concentrated in the African sector (0°-40°E), allowing us to determine reliably the frontal ranges and compare them with results of earlier studies (sections 3.3-3.6). The ensuing downstream changes of *T-S* ranges are described afterward.

3.2. Scotia Front

The northern rim of the Weddell Gyre is contiguous with the southern limit of the ACC. Interaction of waters from the Weddell, Scotia, and Bellingshausen Seas, as well as local thermodynamic processes in the southern part of the Scotia Sea, results in formation of a specific zone, dividing the waters of the Weddell and Scotia Seas, namely, the Weddell-Scotia Confluence [*Gordon*, 1967; *Patterson and Sievers*, 1980]. The WSC is bounded from the north by a distinct subsurface front (sometimes surface-manifested too), the Scotia Front (SF), and from the south by a weaker front, the Weddell Front [*Gordon et al.*, 1977b]. Here we consider only the SF, far more conspicuous than its southern counterpart.

The SF is marked by a maximum thermal gradient in the T_{max} core layer (200-700 m) of the Circumpolar Deep Water (CDW). Crossing the SF southward, the T_{max} decreases from 1.5°-2.0°C to below 0.5°C. The CDW S_{max} in the 800-to-1200-m layer decreases southward across the SF, from 34.70-34.72 to 34.67-34.68. In the surface layer, the SF is often indistinct. In the T_{min} layer, the SF is manifested as a thermal front, across which the T_{min} decreases southward from 0°-0.5°C to below -1.0°C.

Analysis of many sections across the SF [*Belkin*, 1993a] shows that the 1°C isotherm in the 300-to-500-m layer is a fair indicator of the SF axis, being virtually coincident with or very close to the latter. It is this criterion that was used in the present work to pinpoint the front location.

3.3. Polar Front

A summary of criteria for identification of the PF is given in Table 1.

Consistency of these definitions was debated for decades [*Gordon*, 1971; *Patterson and Sievers*, 1979/1980; *Deacon*, 1982]. We used *Botnikov*'s [1963] criterion for three reasons: (1) The 2°C isotherm is a good approximation of the northern extent of the subsurface T_{min} almost everywhere in the Southern Ocean. An exception is a limited area in the SE Pacific, where the PF is located far to the south, at 62°-63°S, with correspondingly colder T_{min} [*Gordon*, 1971; *Emery*, 1977]. Another peculiar area is the northernmost part of the Kerguelen Plateau, where as is shown in this work, the T_{min} is slightly warmer, up to 2.5°C. (2) In winter the 2°C isotherm extends vertically up to the surface, providing a reliable indication of the PF location in the absence of the PF's cold-core rings with T_0<2°C shed to the north, in which case Botnikov's criterion would place the front erroneously far north whereas *Deacon*'s [1933] and *Gordon*'s [1971] criteria would be better. (3) Generally, this definition is in conformance with the *Gordon* [1971] definition of the PF as the location of rapid descent of the T_{min}, which reflects the baroclinic nature of the PF.

Surface signatures of the PF, though shifted southward in the summer [*Botnikov*, 1963], could be used as well for the front tracing. In the African sector, the average T_0 range is 2.5°-4.1°C [*Lutjeharms and Valentine*, 1984], while in the Crozet Plateau area this range is 4.1°-5.7°C [*Belkin*, 1989b].

Despite significant meridional displacements, the PF's temperature and salinity vary relatively little throughout the study area. The same temperature criterion, the northern terminus of the 2°C isotherm demarcating the T_{min} in the 100-to-300-m layer [*Botnikov*, 1963], works as well at 58°S as at 48°S. The only exceptional area is the northernmost PF location in the Southern Ocean, namely, the northern flank of the Kerguelen Plateau, where the PF is situated at 46°-47°S. Here the northern terminus of the Antarctic Winter Water is slightly warmer, with the T_{min} up to 2.5°C.

Analyzing 175 PF crossings in 1903-1965, *Buinitsky* [1973] found that within the 14° latitudinal range of the PF in the Southern Ocean (48°-62°S, on average) the PF's axial T_0 range is just about 1°C. While the along-front variability of the surface temperature is small, the seasonal variability is significant. The annual T_0 range is ~2.7°C, being almost independent of latitude, with the minimum (1.6°-2.5°C) in September-October, and with the maximum (4.8°-5.2°C) in February [*Buinitsky*, 1973].

Using the JARE data of 1965-1983, *Belkin* [1988b, 1989b] found that the PF axial surface temperature is 5°C in the Crozet Plateau area and 4°C SW of Australia. This difference may yet be accounted for by the seasonal effect because these JARE data were obtained in March and December, respectively.

3.4. Subantarctic Front

The Subantarctic Front was first identified south of Australia and New Zealand and called the "Australasian Subantarctic Front" [*Burling*, 1961]. *Zillman* [1970] mapped the front from 83° to 164°E. *Emery* [1977] traced this front from Australia up to the Drake Passage and suggested a generic term, the Subantarctic Front. Some clear indications of the SAF's existence and significance can be found already in the work of *Böhnecke* [1936] and *Deacon* [1945]. There is some confusion of the SAF and the STF as noted by *Peterson and Whitworth* [1989]. Only relatively recently has the SAF been fully recognized and studied in all sectors of the Southern Ocean. A summary of its definitions is given in Table 2.

Table 2. Criteria for SAF Identification

Criterion	References
Maximum grad T_0 in the range 5°-9°C	*Burling* [1961]
Axial T_{300}=5-6°C	*Burling* [1961]
Axial T_0=8°C	*Burling* [1961]
Axial S=34.4-34.5 at 100-400 m	*Burling* [1961]
Enhanced subsurface horizontal grad T between the 3° and 5°C isotherms	*Sievers and Emery* [1978]
Axial T_{200}=5°C	*Clifford* [1983]
Rapid descent of the S_{min} to the 500 to 600 m depth	*Whitworth and Nowlin* [1987]
Pronounced subsurface S_{min} north of the SAF	*Whitworth and Nowlin* [1987]
Maximum grad T in the range 3°-8°C at 100-400 m	*Belkin* [1988a]
Axial T_{100}=7°C	*Nagata et al.* [1988]
Origin of the intermediate S_{min} north of the SAF	*Peterson and Whitworth* [1989]
Axial T_{200}=4°C	*Peterson and Whitworth* [1989]; *Orsi et al.* [1993]
Location where the S_{min} layer crosses the 400 to 600 m depth range (about halfway through its descent)	*Patterson and Whitworth* [1990]
Thick, nearly homogeneous layer extending to depths of >=400 m, just north of the SAF	*Patterson and Whitworth* [1990]
T-S ranges of 4°-8°C and 34.1-34.5 at 200 m, with axial values of 6°C and 34.3	*Park et al.* [1993]
S<34.20 at Z<300 m, farther south; T>4°-5°C at 400 m, farther north; O_2>7 mL L^{-1} at Z<200 m, farther south	*Orsi et al.* [1995]

We used primarily the structural criteria, namely the existence of the intermediate S_{min} and the Subantarctic Mode Water (SAMW) thermostad north of the SAF, the latter criterion being applicable only in the eastern part of the study area. A dense database in the African sector (25 sections) allowed us to determine the average T-S ranges of the SAF (Table 3) adjusted downstream to reflect spatial evolution of the front.

From *Lutjeharms and Valentine* [1984], the T_0 range is 5.1°-9.0°C between 20°W and 40°E. At 200 m our T-S ranges compare favorably with those of *Park et al.* [1993]

Table 3. Average *T-S* Ranges of the SAF in the African Sector (0°-40°E)

Depth, m	*T*, °C	*S*, psu
0	6.8-10.3	33.88-34.36
200	4.8- 8.4	34.11-34.47
400	3.7- 6.1	34.19-34.38
600	3.0- 4.3	34.24-34.28

and differ from those of *Clifford* [1983], *Peterson and Whitworth* [1989], and *Orsi et al.* [1993], whose T_{200} axial values are more suitable elsewhere.

We found the SAF's axial indices to be fairly stable across the ocean, from the African sector (0°-32°E) up to the Australian sector (80°-150°E). At 200, 400, and 600 m the approximate axial *T-S* indices are 7°C/34.3 psu, 5°C/34.3 psu, and 4°C/34.3 psu, respectively, in the African sector, while in the Australian sector they are 7°C/34.3 psu, 6°C/34.45 psu, and 5°C/34.4 psu, respectively.

The north side of the Australian SAF is, however, warmer and saltier than the north side of the African SAF, and these differences increase with depth to ~3°C/0.25 psu at 600 m (compare 4°-5°C/34.3 psu south of Africa and 7°-8°C/34.55 psu south of Australia). This contrast reflects the existence of a thick thermohalostad north of the Australian SAF, and the effect of the STF-to-SAF heat/salt transfer, discussed below. Both phenomena result in the Australian SAF being much stronger and deeper than the African SAF.

Table 4. Criteria for STF Identification

Criterion	References
Winter T_0 range=11.5°-15.5°C; summer T_0 range=14.5°-18.5°C; summer S_0 at the southern edge=34.4	*Deacon* [1933]; *Stramma and Peterson* [1990]; *Stramma* [1992]
North of the STF, winter T_0=11.5°-16.5°C, summer T_0=14.5°-19.5°C, S_0=34.9-35.5	*Deacon* [1937]; *Stramma and Peterson* [1990]; *Stramma* [1992]
Winter T_0 range=8°-12°C, summer T_0 range=12°-16°C	*Deacon* [1960]
S_0 range=34.6-35.1; axial S_0=34.9	*Deacon* [1982]
Position of the 26.8 isopycnal at 200 m	*Burling* [1961]
Axial T_{200}=10°C; axial S_0=34.8	*Clifford* [1983]
T_0 range=10°-14°C; axial S_0=34.8	*Whitworth and Nowlin* [1987]
Axial T_{150}=12°C	*Nagata et al.* [1988]
Axial T_{200}=12°C	*Orsi et al.* [1993]*
T-S ranges of 8°-12°C and 34.6-35.0 at 200 m, with axial values of 10°C and 34.8	*Park et al.* [1993]
T_{100} range=10°-12°C; S_{100} range=34.6-35.0	*Orsi et al.* [1995]

*In this paper the value was misprinted as 14°C (A. H. Orsi, personal communication, 1993).

Table 5. *T-S* Ranges of the North STF in the Central South Atlantic

Depth, m	Side	Cruise and Section					
		SAVE-5 (25°W)		SAVE-4 (7°W)		Ajax (1°E)	
		T, °C	*S*, psu	*T*, °C	*S*, psu	*T*, °C	*S*, psu
0	warm	22.6	35.81	20.6	35.76	16.5	35.60
0	cold	21.3	35.33	18.2	35.15	15.1	35.25
200	warm	14.4	35.46	14.5	35.30	15.3	35.50
200	cold	12.5	35.19	12.7	35.16	13.3	35.25
400	warm	12.2	35.14	11.2	34.96	12.2	35.07
400	cold	9.0	34.68	9.1	34.68	10.3	34.85
600	warm	8.0	34.59	7.3	34.52	8.9	34.69
600	cold	5.5	34.32	5.8	34.33	7.2	34.52

3.5. Subtropical Front

A summary of the STF definitions is presented in Table 4.

In earlier studies a single STF has been identified, although many researchers described this front as a broad Subtropical Frontal Zone (STFZ), up to 4°-5° latitude, that may consist of several cores (fronts) interspersed by zones of relatively homogeneous waters [e.g., *Shannon et al.*, 1989; *Lutjeharms et al.*, 1993].

Analyzing the South Atlantic archive data, *Belkin* [1993a, 1994] distinguished the STFZ's boundaries as the North and South STF (NSTF and SSTF, respectively), extending from the Brazil Current to the Agulhas-Benguela area. His database included sections occupied by *Thomas Washington* (Marathon 8; 40°-42°W), *Vozrozhdenie* (cruise 15; 17°-20°W), *Knorr* (Ajax; 1°-11°E), *Professor Vodyanitsky* (cruise 5; 0°E), *Novoukrainka* (cruise 7; 6°-17°E), *Wilkes* (10°E), *Professor Vize* (cruise 32; 10°E), *Meteor* (cruise 11/5; 11°E), and some surface temperature and salinity data.

A similar STFZ bordered by the NSTF and SSTF was found also in the South Pacific based on five crossings between New Zealand and 126°W made during *Dmitry Mendeleev* cruise 34 [*Belkin*, 1988a](see also *Vinogradov and Flint* [1986] for an English-language summary of the cruise), although these STFZs differ quantitatively.

The double structure of the South Atlantic STFZ is corroborated by data of two South Atlantic Ventilation Experiment (SAVE) sections by *Melville*. The western section (SAVE 5, February 1989) crossed the NSTF (called the "Brazil Current Front" by *Tsuchiya et al.*[1994]) at 34°S, 25°W, and the SSTF (called the "Subtropical Front" by *Tsuchiya et al.*[1994]) at 41.5°S, 28°W. The eastern section (SAVE 4, December 1988 to January 1989) crossed the NSTF (called the "Benguela-South Atlantic Front" by *Gordon et al.*[1992]) at 34°S, 7°W, and the SSTF (called the "Subtropical Front" by *Gordon et al.*[1992]) at 38°S, 11°W. Farther east, the *Knorr*/Ajax 1°E wintertime section (October 1983) crossed

Table 6. *T-S* Ranges of the South STF in the Central South Atlantic

Depth, m	Side	Cruise and Section					
		SAVE-5 (25°W)		SAVE-4 (7°W)		Ajax (1°E)	
		T, °C	*S*, psu	*T*, °C	*S*, psu	*T*, °C	*S*, psu
0	warm	17.1	35.14	17.6	35.27	14.3	35.17
0	cold	13.5	34.32	15.3	34.78	10.7	34.42
200	warm	12.5	35.23	12.3	35.10	13.0	35.18
200	cold	6.9	34.42	10.4	34.86	8.8	34.54
400	warm	7.9	34.54	9.2	34.72	10.3	34.85
400	cold	4.5	34.21	7.5	34.50	5.8	34.33
600	warm	4.8	34.25	5.6	34.32	6.6	34.44
600	cold	3.4	34.19	4.8	34.26	4.0	34.22

the NSTF at 35.5°S and the SSTF at 37°-40°S. Combined (Tables 5 and 6), these high-quality data confirm zonal continuity of the NSTF and SSTF across the South Atlantic and a clear distinction between the fronts.

In the present work the NSTF in the SE Atlantic is identified by a sharp change of S_0 across 35.5, combined with a sharp change of T_0 across 20.0°C (in summer), both criteria being consistent with the central South Atlantic data (Table 5). The SSTF in the African sector (0°-40°E) is identified by the existence of the subsurface S_{max} south of the front, plus a sharp change of S_0 across 35.0. The average *T-S* ranges of the NSTF and SSTF (by 6 and 19 sections, respectively) are given in Tables 7 and 8.

According to *Lutjeharms and Valentine* [1984], across the STF, T_0=10.6°-17.9°C, and S_0=34.3-35.5 [*Lutjeharms*, 1985], so their surface STF is a concatenation of our NSTF and SSTF. The surface STF of *Whitworth and Nowiln* [1987] is actually our SSTF. At 200 m our *T-S* ranges for the SSTF are close to the *T-S* ranges of the STF prescribed by *Park et al.*[1993], while the axial 12°C isotherm defined by *Orsi et al.*[1993] for the STF falls between our NSTF and SSTF. The double STF concept for the South Atlantic/African sector is thus fully consistent with the results of earlier investigators.

This concept is extendable into the South Indian Ocean, where we found a new front, the NSTF (see section 4.5), similar to the NSTFs of the South Atlantic and South Pacific oceans. The South Indian NSTF seems to diverge from the Agulhas Front (described below) east of 55°E.

3.6. Agulhas Front

The Agulhas Front is mainly a subsurface/intermediate front, quite strong and deep beneath the upper 100-150 m. A summary of its definitions is given in Table 9.

Table 7. Average *T-S* Ranges of the North STF in the SE Atlantic (0°-11.5°E)

Depth, m	*T*, °C	*S*, psu
0	14.0-16.9	34.87-35.58
200	12.1-15.3	34.99-35.42
400	9.3-12.2	34.71-35.07
600	6.0- 9.2	34.40-34.73

Table 8. Average *T-S* Ranges of the South STF in the African Sector (0°-40°E)

Depth, m	*T*, °C	*S*, psu
0	10.3-15.1	34.30-35.18
200	8.0-11.3	34.42-34.92
400	6.1- 8.6	34.38-34.63
600	4.2- 5.9	34.30-34.44

In this work we used a new criterion derived from analysis of a group of selected CTD stations bracketing the front south of Africa, obtained in *Knorr* cruise 104-5, *S.A.Agulhas* cruise 48, *Robert D. Conrad* cruise 17, *Islas Orcadas* cruise 12, and *Discovery* cruise 165A. Analysis of numerous sections has shown that the 10°C isotherm, embedded in the AF, has the maximum depth range across the front, from <300 m to >800 m. The 10°C depth (Z_{10}) correlates strongly with the *T-S* indices: if Z_{10}<300 m or Z_{10}>800 m, then these indices are fairly stable and characterize the right and left sides of the AF, respectively, looking downstream. The choice of 10°C isotherm is optimal because this isotherm is also embedded in the main thermocline where the *T-S* dispersion is at minimum [*Gordon et al.*, 1987; *Valentine et al.*, 1993].

The principal criterion of the AF is thus the depth range of the 10°C isotherm, namely Z_{10}=300-800 m (south of Africa, at 16°-27°E). Farther east, this range decreases to ~350-700 m north of the Crozet Plateau and to ~400-650 m in the Kerguelen-Amsterdam Passage, reflecting gradual weakening of the AF (sections 4.4 and 4.5).

We also used a structural criterion of the AF, namely the existence of a thermostad on its warm side, in the 150-to-300 m layer [*Gordon et al.*, 1987]. The thermostad becomes cooler and fresher eastward: from 17°-18°C/35.5-35.6 psu at 20°E to 12°-14°C/35.2-35.4 psu at 70°E. This cooling/freshening could be partially accounted for by the northward leakage of the most warm and salty surface waters of the AF. A part of the leakage waters, east of 55°E, could join the NSTF (section 4.5).

On the basis of the 10°C criterion, we determined *T-S* ranges of the AF using the set of 13 CTD sections south of Africa described above (Table 10). Like other quantitative criteria, these *T-S* ranges are adjusted alongstream in conformance with substantial cooling and freshening of the AF to the east.

Lutjeharms and Valentine's [1984] T_0 range of the AF is 15.7°-21.0°C (at 13.5°-25°E), overlapping with their STF's

Table 9. Criteria for AF Identification

Criterion	Reference
Axial T_{200}=15°C (the flow axis)	*Grundlingh* [1983]
T_{200} range=10°-17°C	*Gordon et al.* [1987]
Warm side 17°-18°C thermostad at 150-280 m	*Gordon et al.* [1987]
Axial T_{150}=18°C	*Nagata et al.* [1988]
T-S ranges of 12°-16°C and 35.1-35.5 at 200 m, with axial values of 14°C and 35.3	*Park et al.* [1993]

Table 10. Average *T-S* Ranges of the AF in the African Sector (16°-27°E)

Depth, m	*T*, °C	*S*, psu
0	18.7-21.7	35.39-35.54
200	10.8-17.7	34.90-35.57
400	7.4-15.2	34.56-35.43
600	4.8-12.5	34.38-35.13

Table 11. *T-S* Indices of the North Side of the AF and Its Extension, the Australian STF

Depth,	AF at 20°-25°E		STF at 120°-130°E	
m	*T*, °C	*S*, psu	*T*, °C	*S*, psu
200	17.3-18.0	35.53-35.61	11.6-12.1	35.02-35.05
400	14.2-16.1	35.38-35.48	9.3- 9.8	34.71-34.83
600	12.1-13.0	35.12-35.22	8.5- 8.8	34.62-34.69

T_0 range (10.6°-17.9°C). Our *T-S* ranges for the AF are distinctly different from those for the SSTF at all specified depths. At 200 m our *T-S* ranges compare favorably with those of *Gründlingh* [1983], *Gordon et al.*[1987], and *Park et al.*[1993], supporting the consistency of the new approach with previous studies.

The temperatures and salinities along the north side AF and its extension, the Australian STF, decrease substantially from 20° to 130°E (Table 11), although the front's latitude remains nearly constant, ~40°S.

4. Frontal Pattern

4.1. Overview

Figure 3 shows all individual frontal crossings, 710 in all. Figure 4 portrays the frontal pattern based on these crossings. Figure 5 displays the full circumpolar frontal scheme that combines the South Indian Ocean frontal positions with those of the South Atlantic and South Pacific sectors [*Belkin*, 1988a, 1993a, 1994]. We will discuss the frontal structure regionally, proceeding eastward from 0° to 150°E (sections 4.2 to 4.7). All principal results are summarized in the conclusions (section 5).

4.2. Central Southeast Atlantic (0° - 10°E)

The frontal structure of the central South Atlantic was poorly known until the 1980s, when the first generalizations emerged. *Lutjeharms and Valentine* [1984] and *Lutjeharms* [1985] investigated *T-S* fronts from 20°W to 40°E, relying mainly upon the Antarctic supply vessels' data. *Gouretski* [1987] mapped the South Atlantic surface thermal fronts using underway data. *Reid* [1989] investigated the total geostrophic circulation and tracers distributions in the South Atlantic. *Stramma and Peterson*

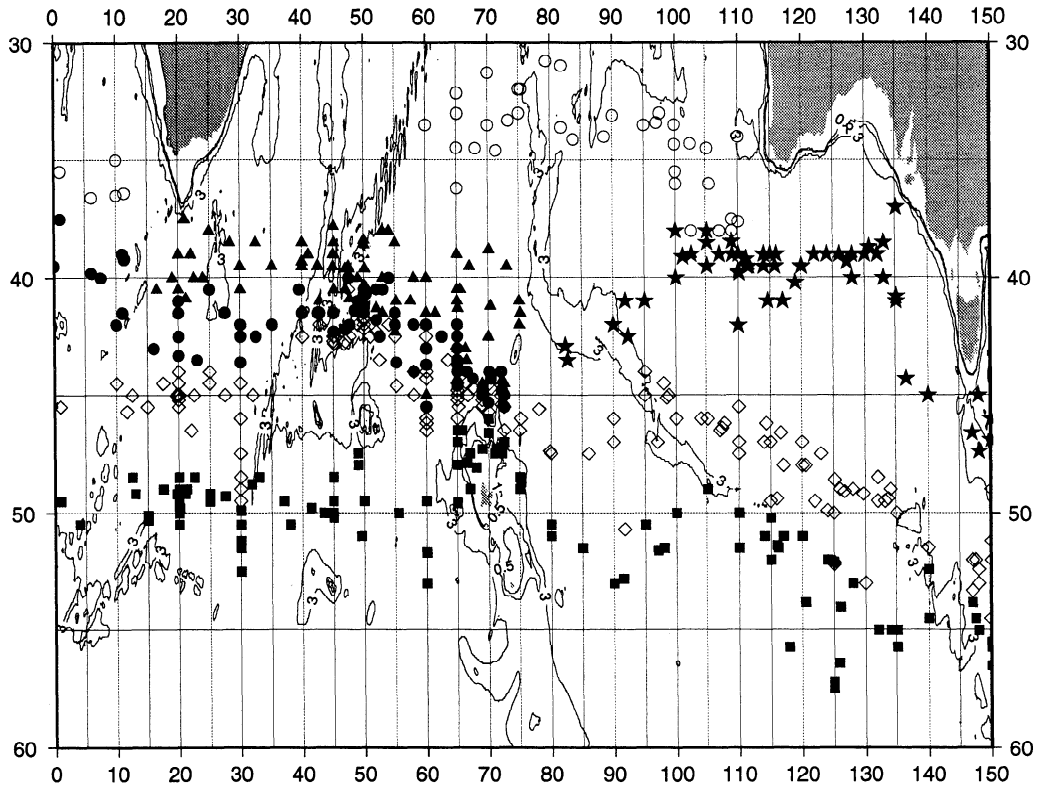

Figure 3. Locations of front centers on individual frontal crossings (710, in all). The fronts are (from north to south) the North Subtropical Front (open circles), the Agulhas Front (triangles), the South Subtropical Front in the Australian sector (stars) and in the African sector (solid circles), the Subantarctic Front (diamonds), and the Polar Front (squares).

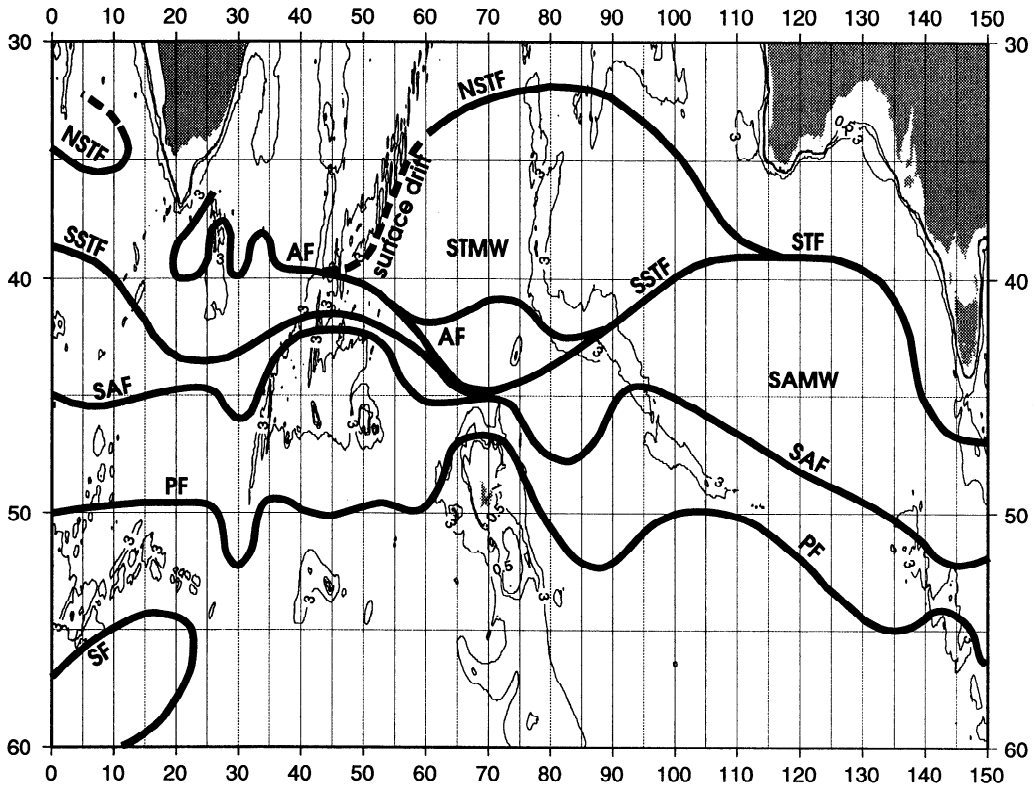

Figure 4. Frontal pattern from 0° to 150°E. Shown are the North and South Subtropical fronts (NSTF and SSTF, respectively), the Agulhas Front (AF), the Subantarctic Front (SAF), the Polar Front (PF), and the Scotia Front (SF). In the Crozet Basin (60°-85°E), two alternative paths of the AF are shown (discussed in section 4.5). In the Australian sector the SSTF is termed the STF downstream of its confluence with the NSTF (110°-115°E). The Subtropical and Subantarctic Mode Water areas are roughly indicated by STMW and SAMW, respectively.

[1990] investigated the STF across the entire South Atlantic. *Peterson and Stramma* [1991] presented an extensive literature survey of the South Atlantic climate, upper layer circulation and meridional heat transport. *Belkin* [1993a, 1994] analyzed all available published data on frontal crossings in the South Atlantic and distinguished NSTF and SSTF (section 3.5), the SAF, the PF, and the SF (Figure 5). *Stramma and Peterson* [1990, p. 851] noted "secondary temperature and salinity fronts" near the STF, but their frontal scheme contains a single STF only.

The frontal structure of the central southeast Atlantic as shown by Figure 6 (*Knorr*/Ajax 1°E section [*Whitworth and Nowlin*, 1987]) includes the NSTF at 35°-36°S, the SSTF at 37°-40°S, the SAF at 45°-46°S, the PF at 49°-50°S, and the SF at 55°-57°S. Poleward of the SSTF, the subsurface S_{max} extends nearly to the SAF. The distinct S_{min} emerges north of the SAF, sinks, and continues northward at intermediate depths. There are no appreciable quantities of SAMW [*McCartney*, 1977] north of the SAF, above the S_{min}. The distinct Antarctic subsurface T_{min} terminates abruptly at the PF and cannot be discerned north of the PF on this section.

4.3. South African Sector (10° - 35°E)

The frontal structure of the African sector is the most diverse [*Lutjeharms*, 1985; *Lutjeharms and Valentine*, 1984; *Gordon et al.*, 1987]. The following fronts are situated here: the AF, the NSTF, the SSTF, the SAF, the PF, and the SF. The last three fronts are easily discerned given an adequate station spacing. The AF and the SSTF, however, are close to each other and could join occasionally.

In this work we used the 10°C depth criterion (section 3.6) that allowed us to distinguish the AF from the SSTF on each section that crossed both fronts and to show that the AF and the SSTF are distinct, separable fronts that can be traced individually all the way from the Agulhas Retroflection to 52°E, and sometimes up to 75°E, through the Kerguelen-Amsterdam Passage.

The AF interacts with the subantarctic waters that frequently spread northward in cyclonic meanders and rings; a particularly strong and persistent meander of the AF is observed regularly over the Agulhas Plateau, centered at 26°E [*Lutjeharms and Van Ballegooyen*, 1984, 1988]. Another quasi-stationary meander is observed downstream of the Agulhas Plateau, at 32°-33°E [*Lutjeharms and Van Ballegooyen*, 1988; *Quartly and Srokosz*, 1993].

The AF interacts also with the SSTF. Our results (Figures 3-4) show a southward deflection of the SSTF impinging on the Agulhas Retroflection. To some extent, both the Agulhas Retroflection and the turn in the SSTF may be influenced by the Schmitt-Ott Seamounts situated in between, at 39°26'S, 13°45'E.

The final fate of the NSTF of the South Atlantic is

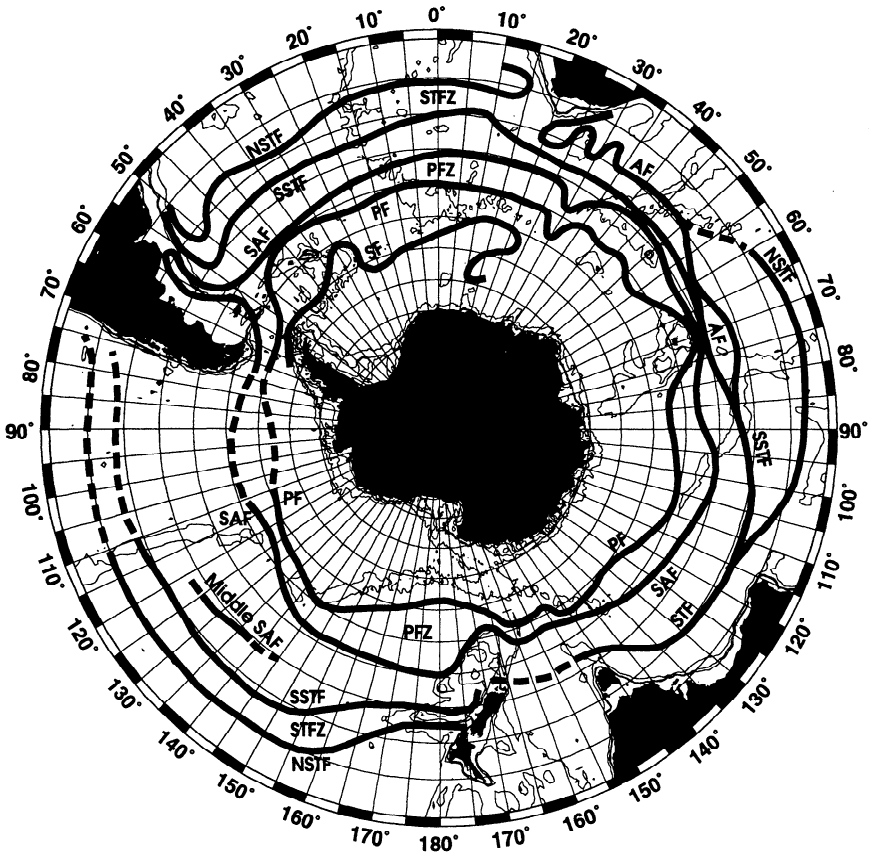

Figure 5. Southern Ocean frontal scheme based on this study (0°-150°E), *Belkin* [1993a, 1994] (the South Atlantic), and *Belkin* [1988a] (the South Pacific). Shown are the North Subtropical Front (NSTF), the South Subtropical Front (SSTF), the Agulhas Front (AF), the Subantarctic Front (SAF), the Polar Front (PF), and the Scotia Front (SF). South of Australia, the single Subtropical Front (STF) is shown. The Subtropical Frontal Zone and Polar Frontal Zone are marked by STFZ and PFZ, respectively. The Antarctic Zone is to the south of the PF. Dashed lines show poorly defined frontal positions.

unclear. This front can blend with the SSTF, the AF, or both. Alternatively, the NSTF can bend northward (into the Benguela Current?)[*Gordon and Bosley*, 1991, Figure 3].

The frontal structure of the eastern part of the South African sector is clearly seen in the *Fiolent* cruise 21 30°E section (Figure 7). The southern part of this transect resembles the *Discovery* cruise 164 32°E section [*Read and Pollard*, 1993, Figure 3]. In both cases the PF is very strong, probably as a result of the confluence with the SAF [*Read and Pollard*, 1993], which apparently bends sharply southward along 30°E, upstream of its encounter with the Mid-Ocean Ridge (Figures 3-4). For example, in the *Fiolent* section (Figure 7) the SAF is shifted to 49°S, where it joins the PF. The average position of the SAF at 30°E is 47°S (Figures 3-4). However, farther downstream, the SAF turns northeast, following the western flank of the ridge, and joins the SSTF north of the Crozet Plateau.

The PF loops southward along ~30°E after crossing the Mid-Ocean Ridge (Figures 3-4). The anticyclonic meandering of the PF in this area has been noted also by *Orsi et al.* [1993] and *Gouretski and Danilov* [1993]. Enhanced mesoscale variability apparently associated with the PF's meanders and warm rings, that form after the PF crosses the Mid-Ocean Ridge, is clearly seen in the Geosat altimeter data [*Sandwell and Zhang*, 1989; *Chelton et al.*, 1990; *Quartly and Srokosz*, 1993].

4.4. Crozet Plateau Area (35° - 60°E)

The Crozet Plateau area is featured by the confluence of several fronts. The SAF is deflected northward, presumably by the bottom relief, and converges with the SSTF north or northeast of the Prince Edward Islands. The frontal structure of the western part of this region is displayed on *Professor Mesyatsev* 45°E sections (Figures 8-9). Both sections, especially the former, show the AF well apart from the SSTF/SAF. The AF's position is variable, from 38°-39°S to 40°-41°S. The latter section shows also the PF at 49°S, south of the Crozet Plateau.

East of 50°-52°E, the AF joins the SSTF/SAF to form a triple AF/SSTF/SAF (Figures 10a and 10b). This front is referred to as the "Crozet Front", which is quite accurate in the geographical sense because this phenomenon occurs within the Crozet Basin. The Crozet Front stands as one of the strongest fronts in the world ocean, with the surface *T-S* ranges reaching 11°C/1.8 psu, from 9°C/33.7 psu to 20°C/35.5 psu [*Belkin*, 1988b, 1989a,b, 1990]. The confluence of the AF with the SSTF/SAF seems transient, as the AF was repeatedly observed apart from the SSTF/SAF (Figure 10c,d).

The only source of regular information about this region is French and Japanese supply vessel voyages. The surface temperature data of *Gallieni* allowed *Delépine* [1963] to

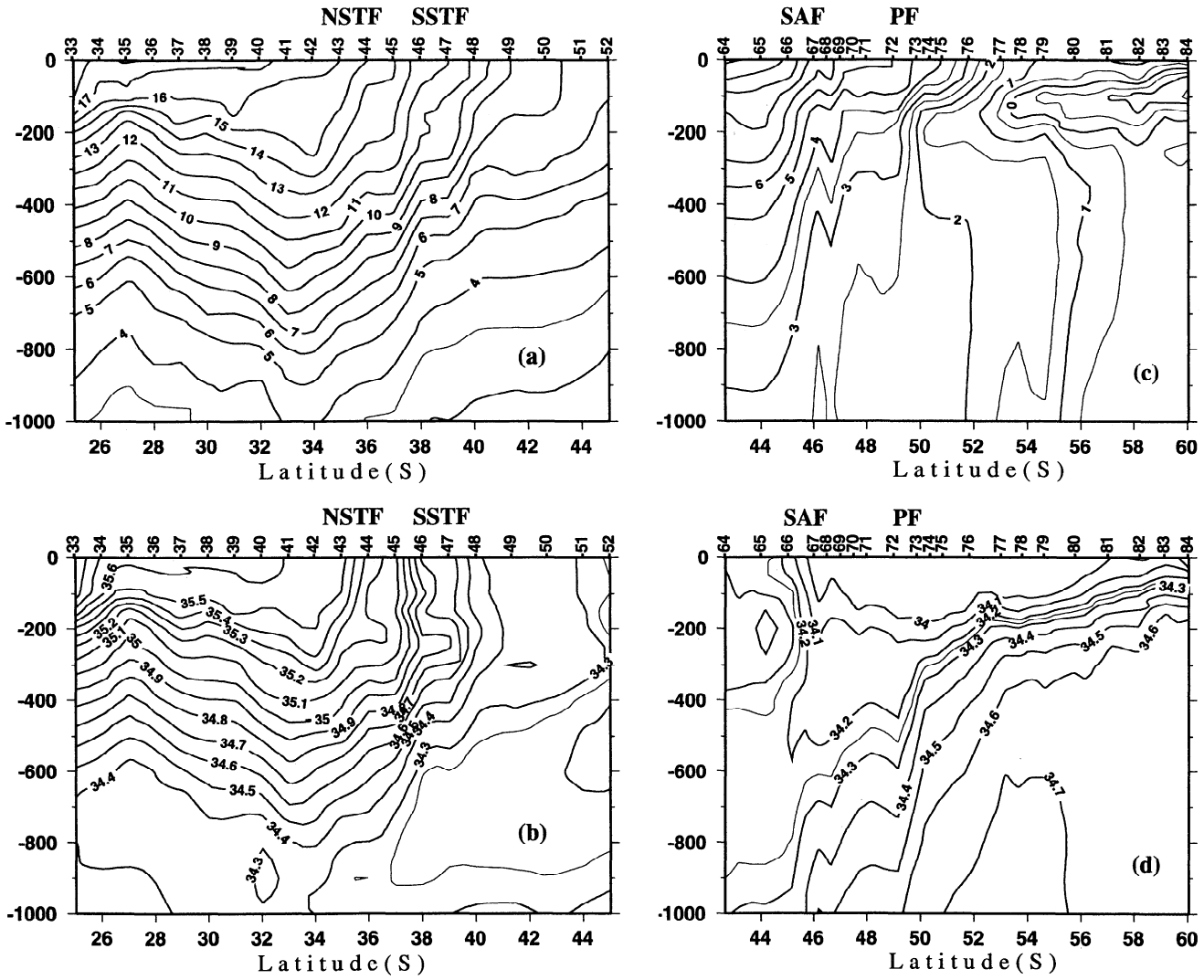

Figure 6. *Knorr*/Ajax section along 1°E: (a) potential temperature (°C) and (b) salinity (psu) for leg I, October 1983, and (c) potential temperature (°C) and (d) salinity (psu) for leg II, January 1984.

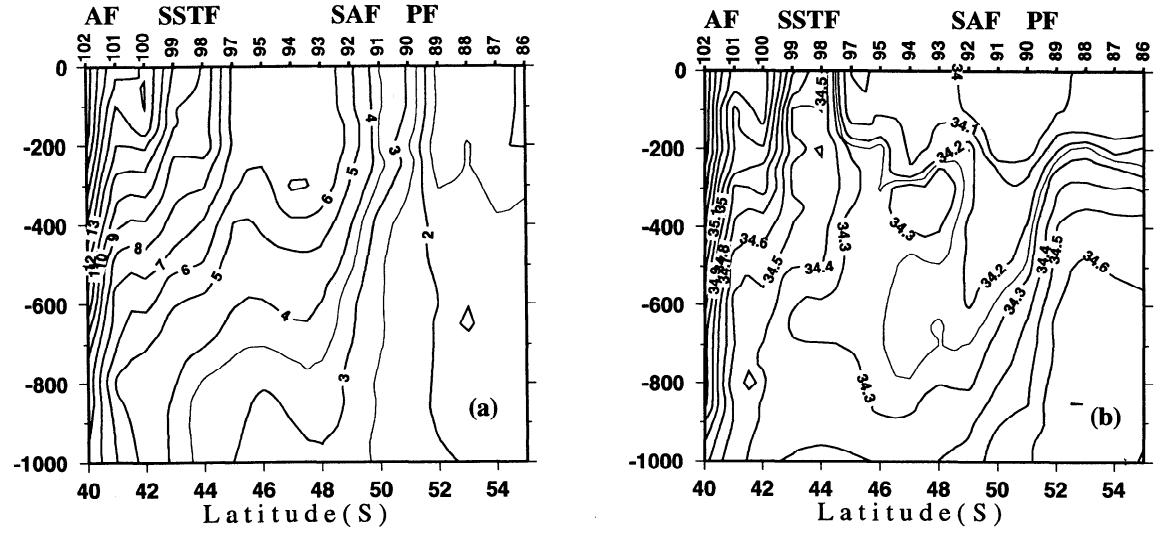

Figure 7. *Fiolent* cruise 21 section along 30°E, July 1987: (a) potential temperature (°C) and (b) salinity (psu).

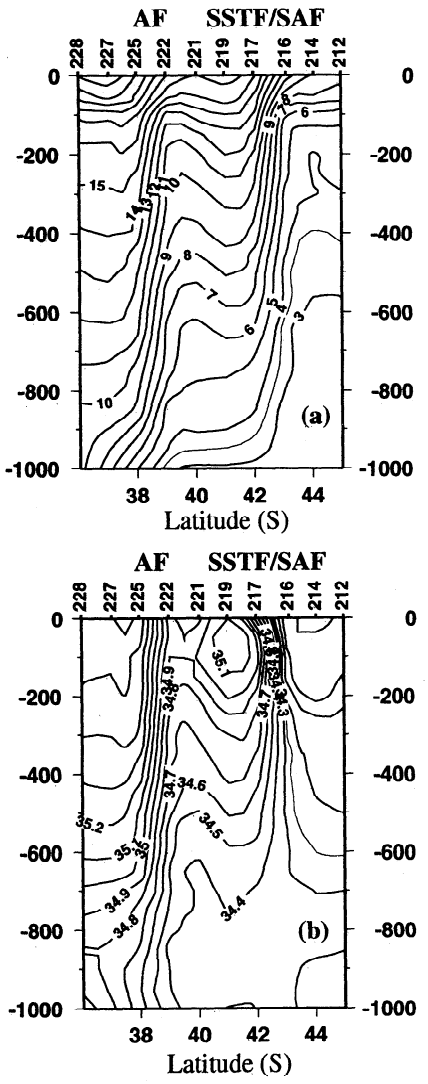

Figure 8. *Professor Mesyatsev* cruise 7 section along 45°E, February 1977: (a) potential temperature (°C) and (b) salinity (psu).

describe a sharp discontinuity north of the Crozet and Kerguelen Plateaus. *Gambéroni et al.* [1982], analyzing XBT and station data of *Gallieni* and *Marion Dufresne*, plus some historical station data, were the first to interpret this discontinuity as a confluence of two fronts, namely, the "Subtropical Convergence" and the "Antarctic Convergence," believing that the latter rounds the Crozet Plateau from the north. They did not mention the SAF at all.

The first analyses of the JARE data in this area were performed by *Nagata et al.* [1988] and *Belkin* [1988b, 1989b, 1990]. *Nagata et al.* [1988] noted the closeness of the SSTF and the SAF north of the Crozet Plateau; however, they did not recognize the confluence of these fronts. *Belkin* [1988b, 1989b, 1990], using the JARE data, identified the SSTF/SAF confluence north of the Crozet Plateau and termed it the "United STF/SAF."

Following J. R. E. Lutjeharms in his identification of the SSTF with the AF east of 30°-35°E, *Nagata et al.* [1988] and *Belkin* [1988b, 1989b, 1990] did not try to distinguish the AF from the SSTF north of the Crozet Plateau. However, the data themselves allow us to discern these two fronts and in the present work we were able to do so. Thus using the results by *Belkin* [1988b, 1989b, 1990] on the SSTF/SAF north of the Crozet Plateau, his term "STF/SAF" should be replaced with "AF/SSTF/SAF" or "Crozet Front."

The first unequivocal identification of the AF north of the Crozet Plateau and its confluence with the ACC at the entrance of the Crozet Basin has been reported by *Park et al.* [1991, 1993]. However, a fine XBT section by *Shirase*/JARE-28 across the central part of the Crozet Plateau [*Michida and Inazumi*, 1988] again shows the AF to be clearly separated from the SSTF/SAF.

In the latest study by J. R. E. Lutjeharms and J. M. Meeuwis (manuscript in preparation, 1995) the surface AF was traced up to 55°E, where it was still seen 30% of the time. These authors used the T_0 range=10°-17°C for the SSTF (plus locational and gradient criteria), while no range criterion was prescribed for the AF, which was

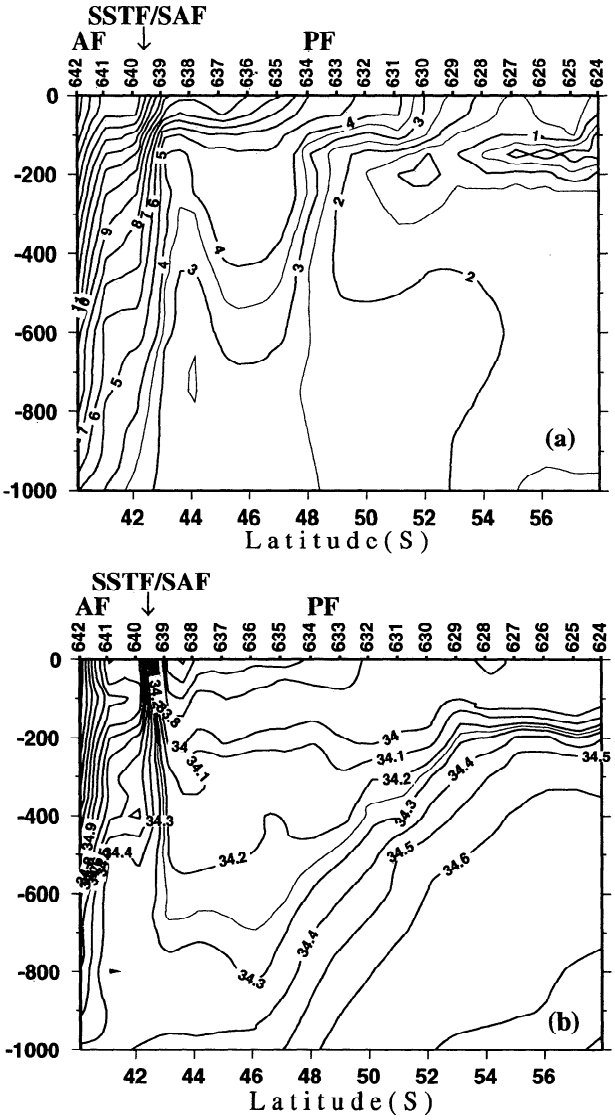

Figure 9. *Professor Mesyatsev* cruise 22 section along 45°E, March 1990: (a) potential temperature (°C) and (b) salinity (psu).

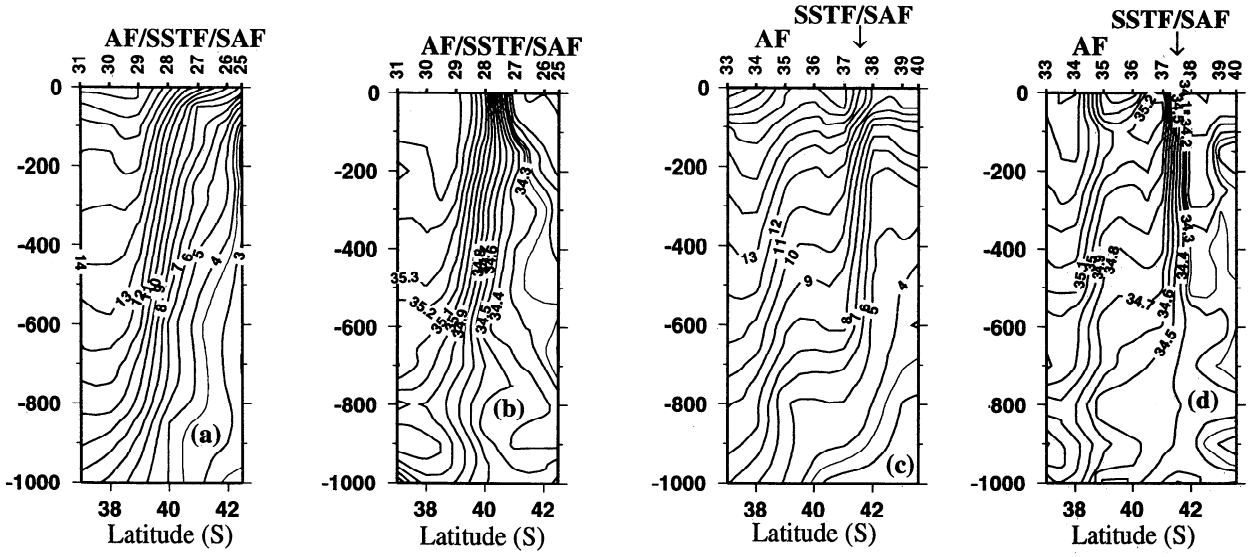

Figure 10. *Geroevka* cruise 6 sections: (a) potential temperature (°C) and (b) salinity (psu) along 50°E, February 1983, and (c) potential temperature (°C) and (d) salinity (psu) along 55°E, March 1983.

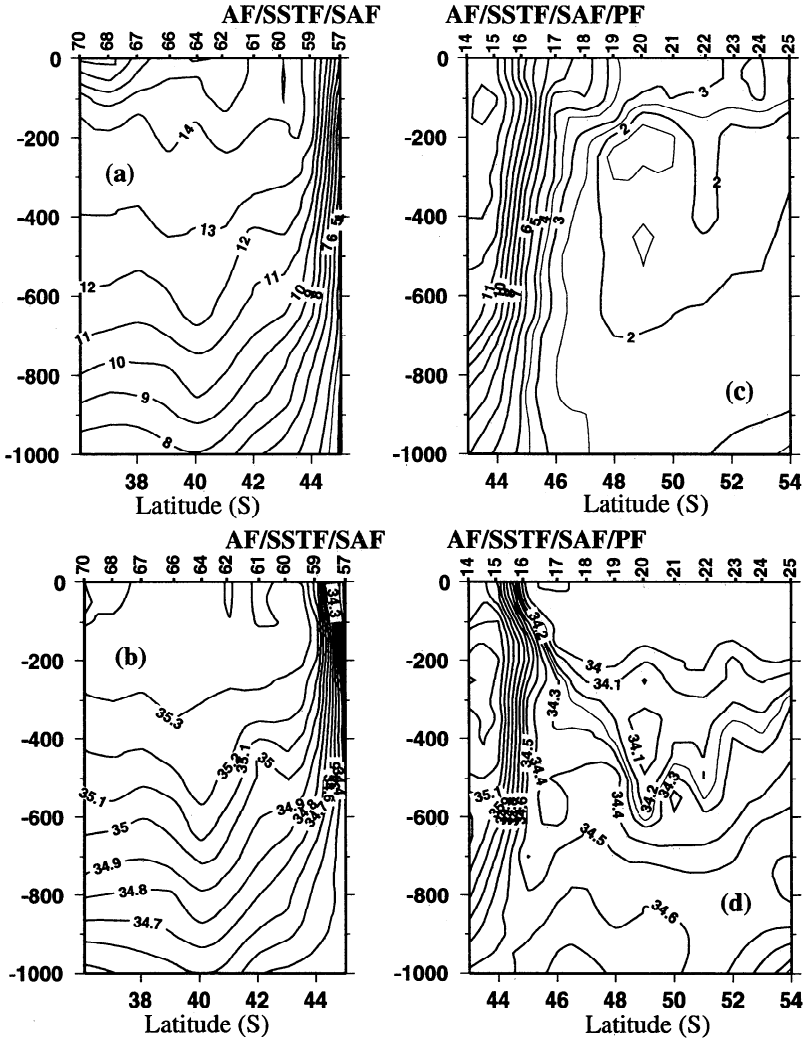

Figure 11. (left) *Professor Mesyatsev* cruise 7 section along 65°E, January 1977: (a) potential temperature (°C) and (b) salinity (psu). (right) *Kara-Dag* cruise 4 section along 72°E, April 1973: (c) potential temperature (°C) and (d) salinity (psu).

identified just as a front that was clearly separate and distinguishable from the SSTF (referred to as "STC") and that had a horizontal gradient of 1°C/18 km to 1°C/80 km (J. R. E. Lutjeharms, personal communication, 1994).

Taking into account that (1) the AF is mainly a subsurface/intermediate front with relatively weak surface signatures and that (2) the AF joins the SSTF in the Crozet Basin [*Park et al.*, 1993; *Belkin and Gordon*, 1993], there is no surprise in the apparent disappearance of the AF east of 55°E, while by subsurface criteria, the AF has been traced much farther east, sometimes up to 75°E, through the Kerguelen-Amsterdam Passage [*Belkin*, 1989a; *Belkin and Gordon*, 1993; this study, section 4.5].

East of the Crozet Islands, the Crozet Front shifts southward, reaching 47°S at 60°E. This may be due to a loss of topographic control as the current associated with the front passes into a basin. The abrupt loss of topographic steering may account for the meandering which is so typical for the deep basin between the Crozet and Kerguelen Plateaus. Indeed, all FGGE 1978-1979 surface drifters passing this area exhibited intense meandering or looping, apparently being trapped by eddies [*Garrett*, 1981; *Gambéroni et al.*, 1982]. The eddy kinetic energy distribution maps from the FGGE drifters and from the Seasat altimetry [*Daniault and Ménard*, 1985] display a maximum in exactly the same area. The Geosat altimeter data [*Sandwell and Zhang*, 1989; *Chelton et al.*, 1990; *Quartly and Srokosz*, 1993] also indicate large mesoscale variability of sea level in this basin which seems very important as a possible conduit for the meridional heat/salt transfer between subtropical and subantarctic waters.

The Polar Front in this area is situated between the Crozet Plateau and the Ob-Lena (Conrad) Rise, extending zonally along 49°-50°S up to the Kerguelen Plateau, where the PF is deflected northward by the topography.

4.5. Kerguelen-Amsterdam Region (60°- 80°E)

West and north of the Kerguelen Plateau, the triple AF/SSTF/SAF or Crozet Front was repeatedly observed (*Ariel* cruise 9, *Professor Mesyatsev* cruise 7). The PF location near Kerguelen was debated in many works [*Belkin*, 1989a]. The main question is: Does the PF pass to the north or south of Kerguelen? Due to shallow depths south of Kerguelen, the PF criteria using the descent of T_{min} may be not suitable here [*Deacon*, 1983]. The PF may also be split upstream of Kerguelen into two branches rounding the island from north and south [*Ostapoff*, 1962; *Gordon et al.*, 1978].

Our analysis unambiguously indicates the northern position of the PF near Kerguelen, although the northern terminus of the subsurface T_{min} in the 100-to-300-m layer is slightly warmer here, up to 2.5°C versus 2°C elsewhere. Taking into account the exceptionally low latitude of the PF in this area (up to 46°-47°S), this warming seems quite natural.

The PF may join the Crozet Front, resulting in a quadruple AF/SSTF/SAF/PF (Figures 11-13). Strictly speaking, the most that could be inferred from the available data with 1° latitude resolution is that these fronts are sometimes very close and cannot be separated. Therefore we prefer to speak about "joining" or "confluence" of the fronts without any implication of "mixing" or "blending".

The PF locations in this area were determined by the analysis of individual stations and not by the inspection of contoured sections, which depends on the quality of contouring and sometimes could be misleading. Each station south of the PF shows a well-defined T_{min} layer with T_{min}=2.0°-2.5°C. For example, at station 215 of the *Vityaz II* cruise 4 section (Figure 12) there is the T_{min} layer at 194-243 m with T=2.18°C, while the underlying Upper Circumpolar Deep Water has T_{max}=2.34°C at 778 m, a stratification typical of the Antarctic Zone (south of the PF). Similar structure was observed along all the sections that cross the northern flank of the Kerguelen Plateau. The northward deflection of the PF and associated flow in the vicinity of the Kerguelen Plateau could result from the conservation of the potential vorticity that forces an equatorward deviation of the flow over shallowing depths. A close inspection of Figures 3-4 shows that this principle applied to the PF and other fronts works well elsewhere.

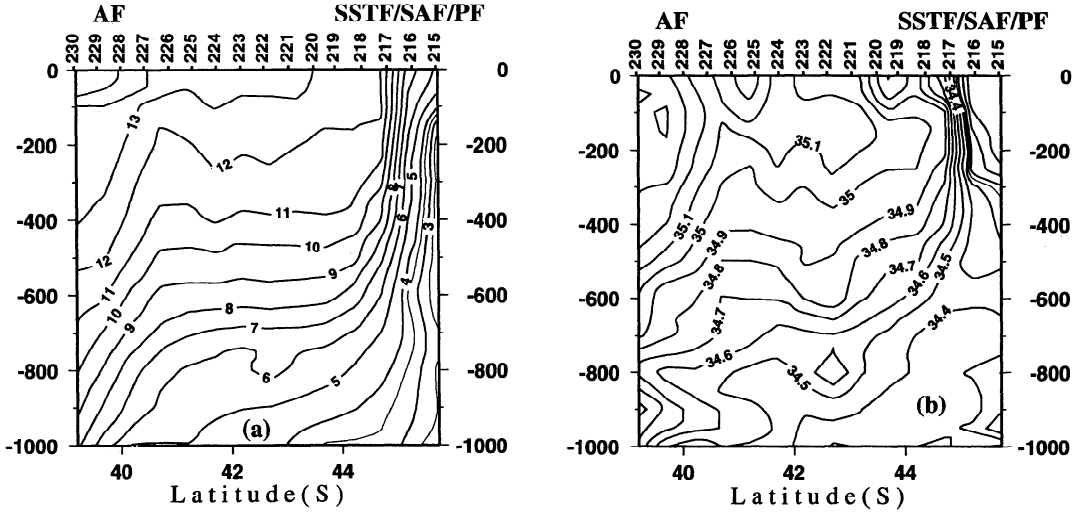

Figure 12. *Vityaz II* cruise 4 section across the Kerguelen-Amsterdam Passage, 67°-73°E, January 1983: (a) potential temperature (°C) and (b) salinity (psu).

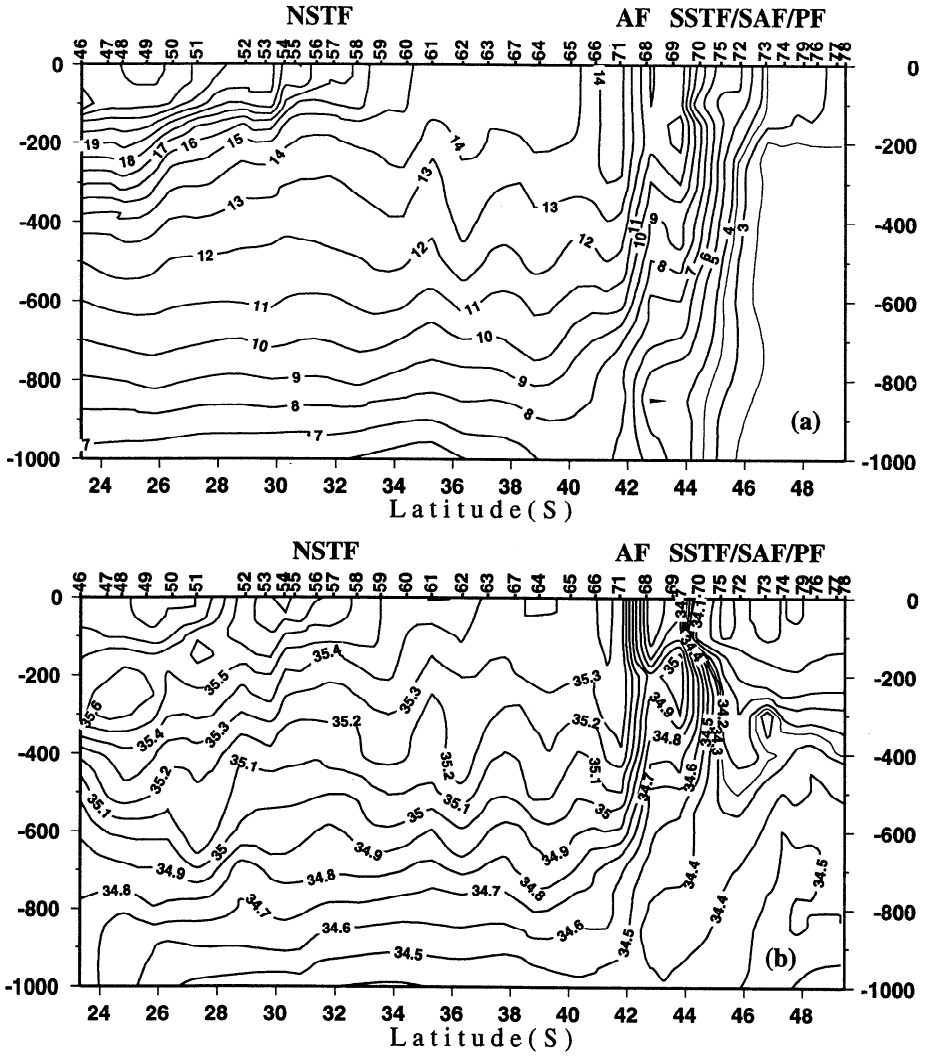

Figure 13. *Yu.M.Shokalsky* cruise 33 leg 1 section along 65°E, July 1976: (a) potential temperature (°C) and (b) salinity (psu).

The PF may be located occasionally well south of Kerguelen [*Klyausov*, 1990]. These displacements, although rare, are very important for biota and fisheries around the Kerguelen and Heard Islands. Generally, the PF is very close to Kerguelen, since the island's climate and biogeography are subantarctic, in contrast with Heard, which is a typical Antarctic island because of its position well south of the PF (see discussion by *Deacon* [1983] and *Belkin* [1989a]).

North of the Kerguelen Plateau, two dominant frontal regimes have been observed. The first regime is represented by the Crozet Front (AF/SSTF/SAF) located in the southern part of the Kerguelen-Amsterdam Passage, usually at 44°-46°S, plus the PF at 46°-48°S. This regime is exemplified by the *Professor Mesyatsev* cruise 7 65°E section and the *Kara-Dag* cruise 4 72°E section (Figure 11), both revealing a distinct 13°C/35.3 psu thermohalostad, a typical feature of the AF's north side. A similar thermohalostad could be seen in other sections cited below. The same feature, though warmer and saltier, could be seen also upstream (Figures 8 and 10). The presence of the thermohalostad on its warm (left) side is the AF's main structural diagnostic signature (section 3.6). The *T-S* parameters of the thermohalostad are changing gradually downstream (section 3.6). In this regime one could expect the splitting of the northernmost part from the Crozet Front downstream of the Kerguelen-Amsterdam Passage and the extension of this branch into the Australian sector as the SSTF.

The second regime differs by the AF, splitting to the north from the Crozet Front, well upstream of the Kerguelen-Amsterdam Passage. This regime is illustrated by the *Vityaz II* cruise 4 section (Figure 12) occupied during Kerguelen-83 survey [*Belkin*, 1989a], when an exceptionally strong, deep (Z_{10}=800 m), separate AF was observed from 64°E up to 72°E [*Belkin and Romanov*, 1990], with the 30 Sv eastward transport relative to 3000 m at 72°E [*Belkin*, 1989*a*]. A distinct, separate AF has been observed here repeatedly, up to 75°E (Figures 13-14). Analysis of the digital data set from the Hydrographic Atlas of the Southern Ocean [*Olbers et al.*, 1992] has also shown the same double-path structure of the AF in the same area, at 60°-80°E [*Sparrow et al.*, 1995, Figure 1]. In the "separated" regime the AF continues along 39°-43°S into the Australian sector, where it is commonly referred to as the STF (we refer to it as the SSTF).

A newly defined front, the North Subtropical Front (NSTF), is distinguished in the range 31°-38°S. This front is the southern boundary of the pool of salty, warm subtropical water of the central South Indian Ocean (e.g., the surface salinity map by *Deutsche Hydrographische Institut* [1960] showing enhanced meridional gradients at the southern periphery of this pool between 75° and 95°E, or the *Akademik Shirshov* cruise 5 70°E section (Figure 14)). The NSTF is likely connected with the AF, diverging from the latter east of 55°E (Figures 3-4). The presence of the NSTF at ~33°S, 60°-90°E, is suggested also by the Fine Resolution Antarctic Model (FRAM) [*Webb et al.*, 1991] as noticed by *Sparrow et al.* [1995].

The South Indian NSTF seems to be a counterpart of similar fronts distinguished in the South Pacific [*Belkin*, 1988a] and in the South Atlantic [*Belkin*, 1993a, 1994] (section 3.5). There are, however, some essential differences between these fronts. For example, the South Atlantic NSTF is fairly deep and strong, with appreciable cross-frontal *T-S* gradients down to at least 600 m, whereas the South Indian NSTF is rather shallow, being limited by the upper 200 (300?) m.

The NSTF is situated just where the wind convergence between westerlies and easterlies is observed [*Hellerman and Rosenstein*, 1983]. The NSTF thus is likely a wind-driven feature, the so long sought "true" Subtropical Convergence. Monthly surface wind data for 1987-1991 [e.g., *Halpern et al.*, 1993] show the wind convergence to be shifted seasonally up to 5° latitude, so one could expect the corresponding shift of the NSTF.

The NSTF is also the northern boundary of the Subtropical Mode Water (STMW) [*McCartney*, 1982] formation region at 60°-100°E, which is bordered on the south by the AF/SSTF and thus encompassed by the two fronts. After bending around the STMW source area, the NSTF proceeds SE, apparently joining the SSTF at 110°-115°E, SW of Australia, to form the Australian STF. It is the influx of the NSTF water that makes the Australian STF appreciably warmer and saltier downstream of the confluence. The southeastward turn of the NSTF is fully consistent with the concept of predominately southward circulation off southwest Australia [*Cresswell*, 1991; *Pearce*, 1991].

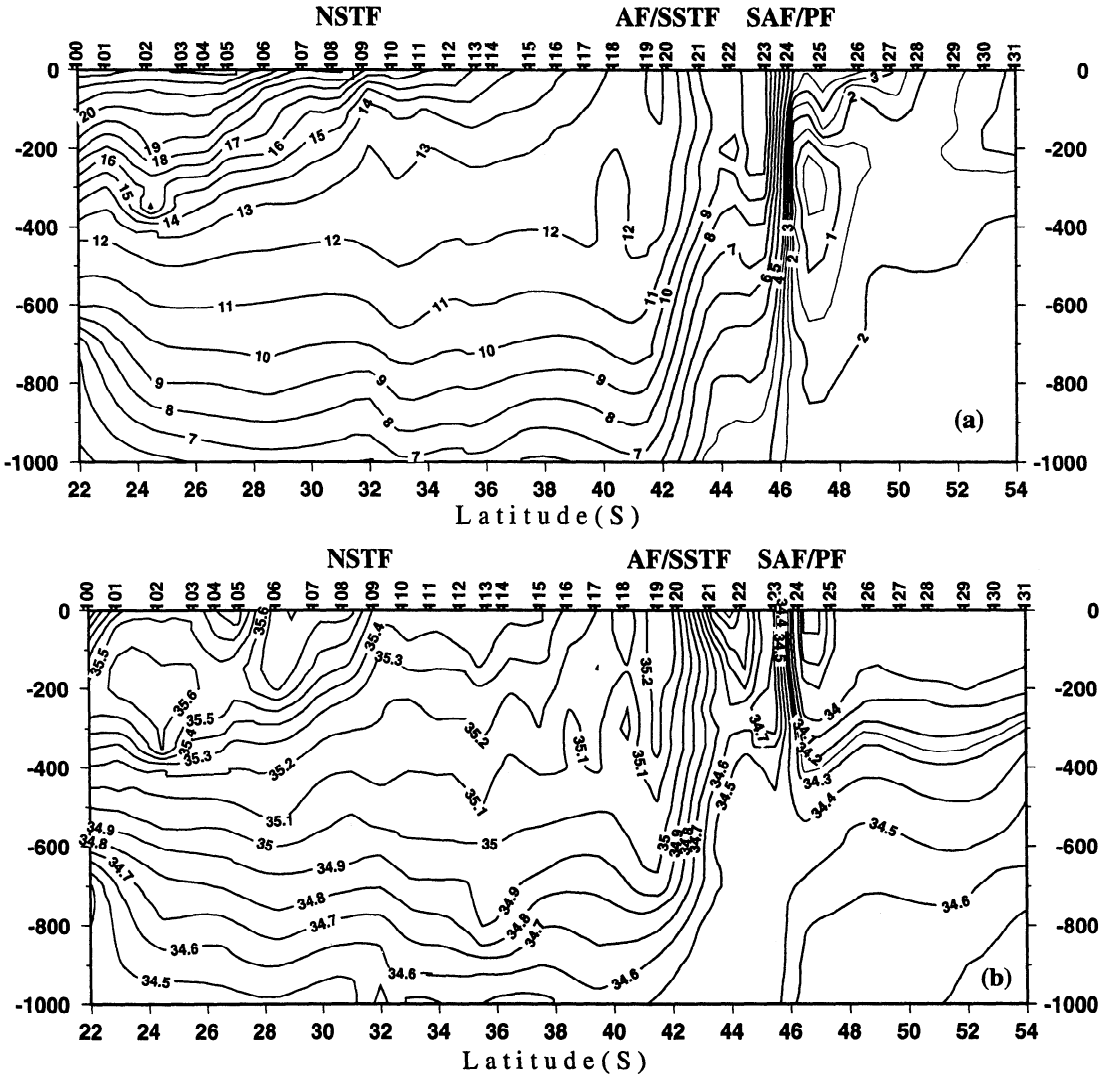

Figure 14. *Akademik Shirshov* cruise 5 section along 70°E, November 1970: (a) potential temperature (°C) and (b) salinity (psu).

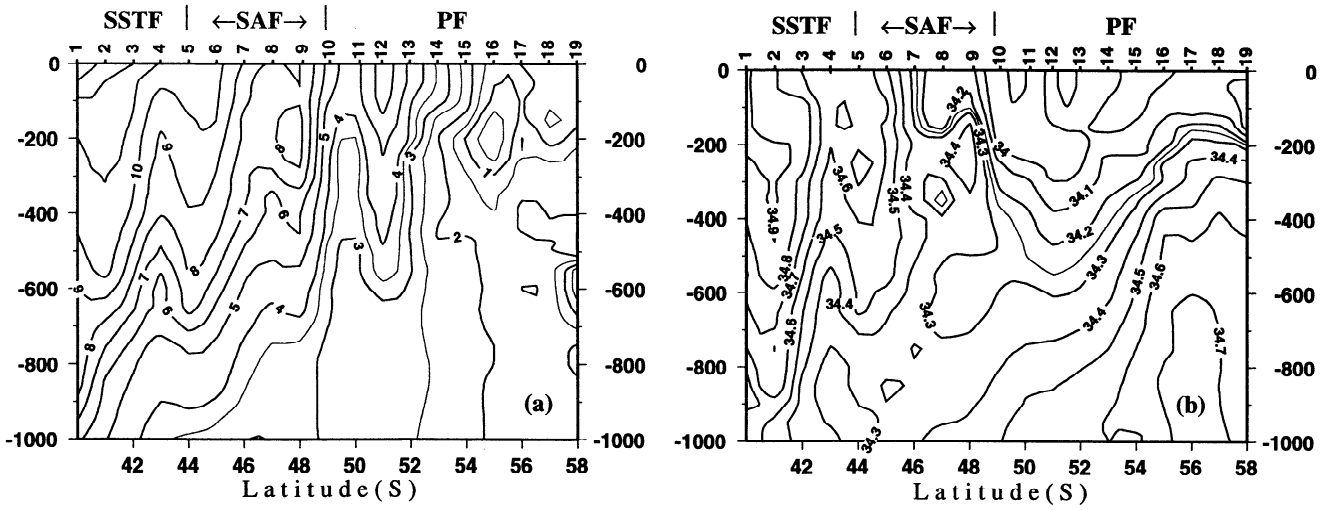

Figure 15. *Kara-Dag* cruise 5 section along 90°E, December 1973: (a) potential temperature (°C) and (b) salinity (psu).

4.6. Southeast Indian Ocean (80°- 115°E)

Downstream of the Kerguelen-Amsterdam Passage, the triple frontal structure (STF, SAF, PF) typical of the Southern Ocean is restored. There are, however, some complications due to front-to-front interactions. For example, the near confluence of the SSTF and the SAF at 90°-95°E may be accounted for alteration of the SSTF and SAF. In the *Kara-Dag* cruise 5 90°E section (Figure 15) the distance between the fairly strong SSTF and the SAF is just 3° latitude, and eddy activity seems vigorous, thus facilitating interfrontal heat/salt exchanges. Enhanced mesoscale variability in this area can be seen in the FGGE drifter data [*Daniault and Ménard*, 1985].

A sharp change of meridional structure takes place between 90° and 110°E as shown by the *Fuji*/JARE-21 110°E XBT section (Figure 16) [*Matsumoto and Mine*, 1982]. The most conspicuous features here are the strong SAF and the extremely thick and homogeneous layer of the 10°-11°C SAMW north of the SAF. The SSTF, north of 40°S, is relatively weak and shallow.

The PF forms a giant poleward meander downstream of the Kerguelen-Amsterdam Plateau, at 80°-95°E. This meander is apparently associated with a distinct maximum of eddy kinetic energy observed in the FGGE drifter data [*Daniault and Ménard*, 1985; *Johnson*, 1989], and with a pronounced high of the sea level mesoscale variability in the Seasat and Geosat altimeter data [*Daniault and Ménard*, 1985; *Sandwell and Zhang*, 1989; *Chelton et al.*, 1990].

4.7. Australian Sector (115°- 150°E)

In the Australian sector the fronts exhibit significant displacements to the south (Figures 3-4). The meridional structure is represented by the *Ob* cruise 1 section from off Adelaide (136°E) to the Davis Sea (93°E) (Figure 17). All three main fronts, the STF, SAF, and PF, are distinct. The

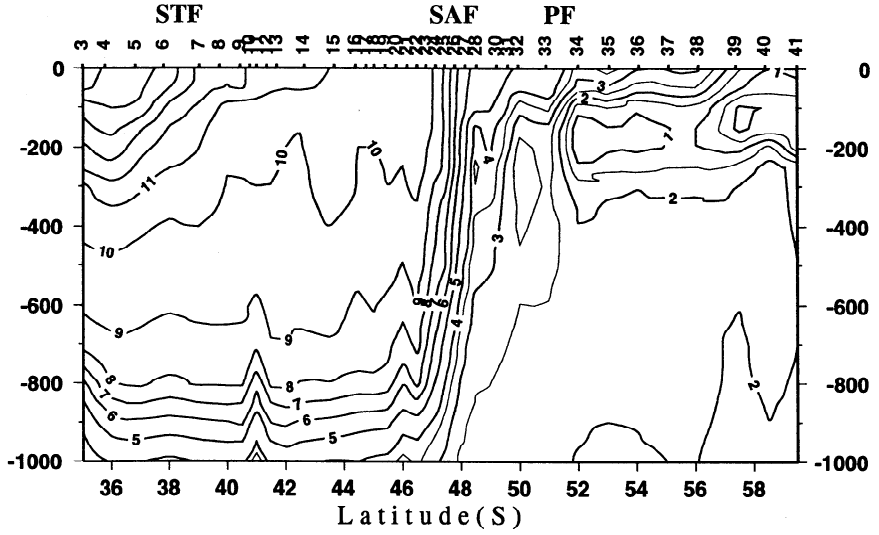

Figure 16. *Fuji*/JARE-21 XBT temperature section along 110°E, December 1979.

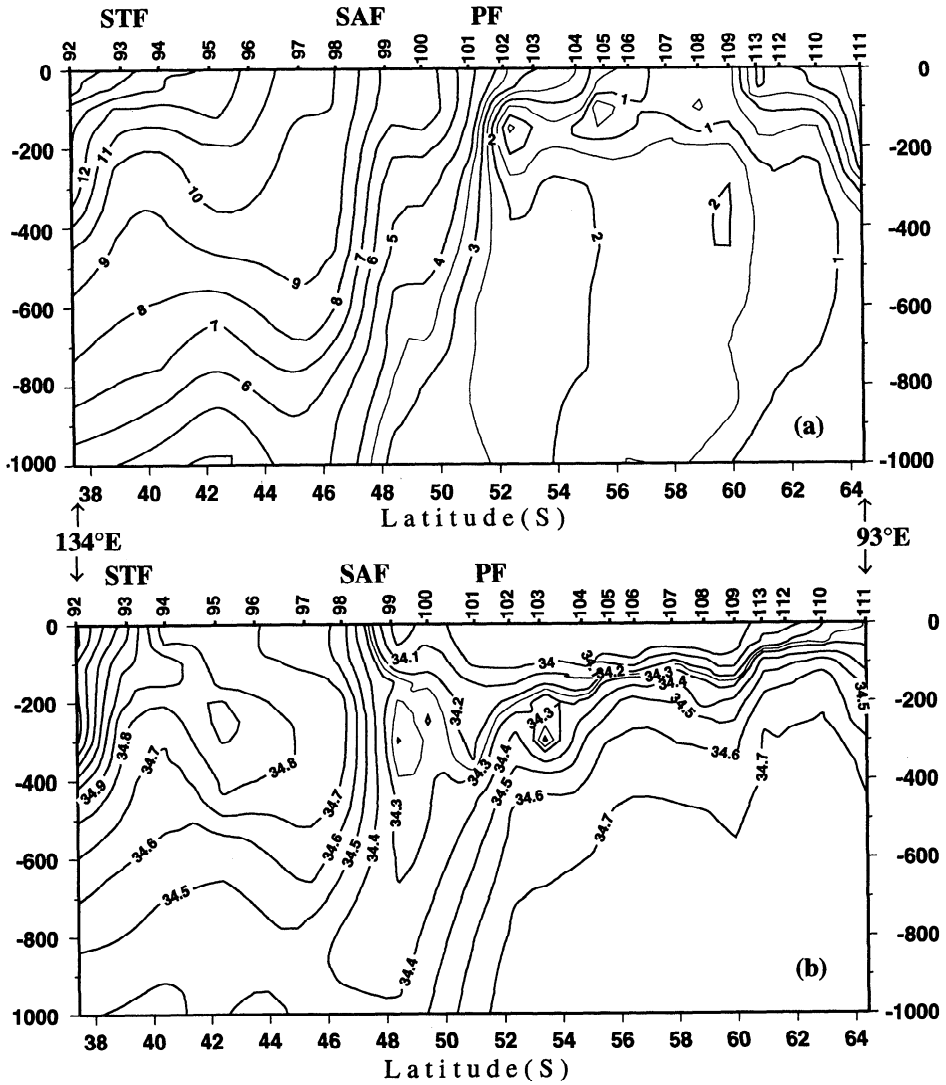

Figure 17. *Ob* cruise 1 section from off Adelaide (134°E) to the Davis Sea (93°E), May 1956: (a) potential temperature (°C) and (b) salinity (psu).

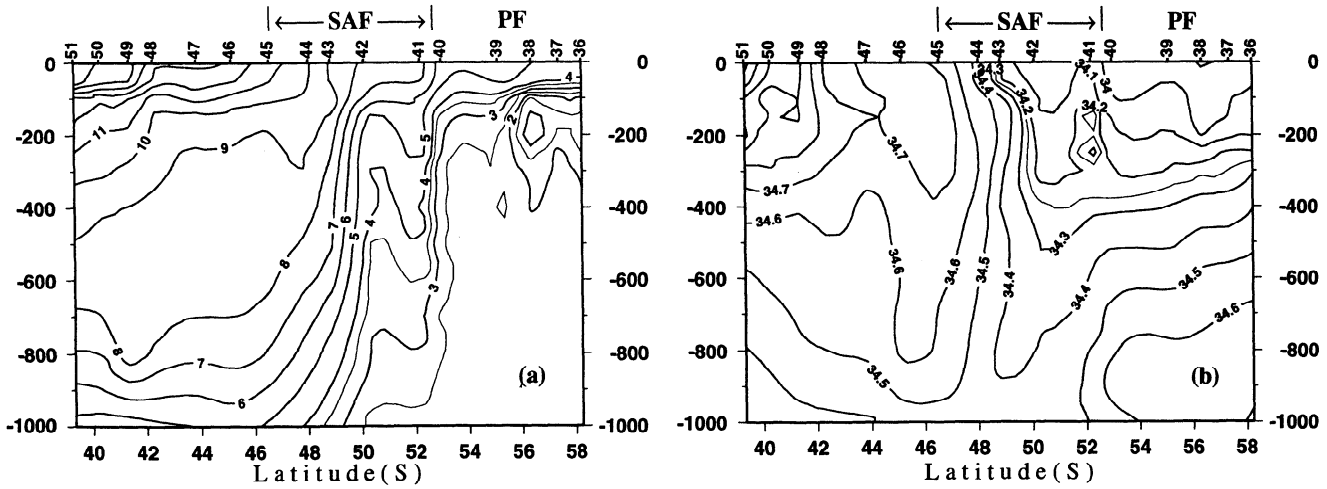

Figure 18. *Zvezda Chernomoria* cruise 4 section along 135°E, March 1983: (a) potential temperature (°C) and (b) salinity (psu).

SAMW (T=9°-10°C, S=34.7-34.8) is colder and fresher than its western counterparts [*McCartney*, 1977]. A subsurface tongue of subtropical water penetrates from the STF into the Subantarctic Zone, a feature typical of the STF.

The central part of this sector was crossed by the *Zvezda Chernomoria* cruise 4 section along 135°E (Figure 18), showing the SAF split into a double front at 47°-50° and 52°-53°S. A similar structure was observed also by *Umitaka Maru* at 116°E [*Matsuura et al.*, 1985]. The "double" SAF and the "double" PF in the Australian sector were observed repeatedly: Figure 3 shows several crossings of the "southern" SAF and the "southern" PF located well south of the main paths of these fronts.

Since the SAF and PF in this sector are ~3° latitude apart, they may join occasionally. Such a confluence was observed at 125°E in *Eltanin* cruise 54. The joined SAF/PF has been repeatedly observed at 147°E, for example, in *Dmitry Mendeleev* cruise 11, and in *Umitaka Maru III* cruise of 1984 [*Matsuura et al.*, 1985]. It is likely, however, that both fronts are still separable at 147°-150°E (as evidenced by two sections by *Volna* cruise 31, one of which is shown in Figure 19), and their apparent confluence may be an artifact caused by wide station spacing.

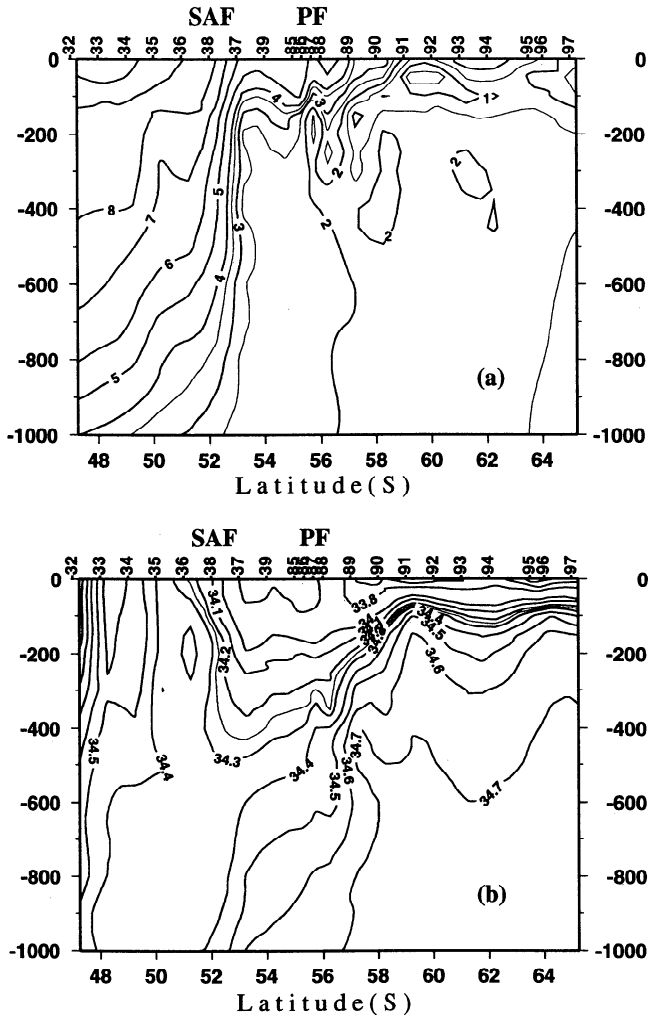

Figure 19. *Volna* cruise 31 section along 150°E, February 1981: (a) potential temperature (°C) and (b) salinity (psu).

5. Conclusions

1. A new, enlarged data set of closely spaced meridional sections, 2°-3° latitude apart, allowed us to trace consistently the main circumpolar fronts from 0° to 150°E and to study their zonal variability. The frontal pattern based on these data (Figure 4) is the first published frontal scheme encompassing the whole Indian sector of the Southern Ocean and elaborated in detail.

2. The AF has been traced from 15°E up to 75°E, through the Kerguelen-Amsterdam Passage, and farther into the SE Indian Ocean as the Australian SSTF. The AF is mainly a subsurface/intermediate front. Its T-S parameters change downstream substantially, thus preventing the use of any fixed isotherm or isohaline for the front tracing. Particularly strong alteration of the AF occurs at 60°-75°E, supposedly due to atmospheric forcing, northward leakage, and the AF/SSTF interaction.

3. The frontal pattern changes dramatically in the SW Indian Ocean, where the AF presses the SSTF to the south, while the SAF, guided by the Mid-Ocean Ridge, turns NE. The SAF joins the SSTF north of the Prince Edward Islands. Farther downstream, in the Crozet Basin at 50°-52°E, the AF occasionally joins the SSTF/SAF to form the AF/SSTF/SAF, referred to as the Crozet Front, which continues to 70°E and branches into the SAF and the SSTF. Alternatively, the AF extends as a separate front across the Crozet Basin through the Kerguelen-Amsterdam Passage and joins the SSTF downstream of the passage.

4. After crossing the Mid-Ocean Ridge at 90°-95°E, the SSTF sharply weakens and shallows, while the adjoining SAF becomes stronger and deeper, supposedly owing to the SSTF-to-SAF transfer of the colder and fresher waters along the Mid-Ocean Ridge.

5. The newly defined North Subtropical Front was distinguished between 31-38°S at the southern boundary of the warm, salty subtropical surface waters. The NSTF is mainly a shallow (200-300 m) haline front, with the S_0 range up to 0.5 psu. At 110°-115°E, the NSTF meets the SSTF to form a single, combined STF.

6. The PF continues zonally between the Crozet Plateau and the Ob-Lena (Conrad) Rise, then turns NE, following the northern flank of the Kerguelen Plateau, sometimes in a close proximity to the SSTF/SAF or AF/SSTF/SAF, thus forming an extraordinary strong front; then the PF returns to the south.

7. In the southeast Indian Ocean the SAF follows the north side of the Mid-Ocean Ridge, while the PF continues along its south side. Both fronts occasionally display a double structure (splitting?) near the Australian-Antarctic Discordance (115°-135°E), possibly due to the loss of topographic control.

Now that we have a detailed description of the South Indian Ocean fronts, we may pose some challenging questions:

1. What happens with the water in between converging fronts? Obviously, this water must sink or be entrained and accelerated by the fronts; however direct observations of these processes are absent as well as observations on

diverging fronts (with upwelling in between?).

2. Why are the fronts so remarkably persistent, retaining their main structural characteristics after merging and splitting? What physics could account for this persistence?

3. How significant is the transport of the modified Agulhas waters along the AF and its extension, the Australian STF? What happens with these waters downstream of the Kerguelen-Amsterdam Passage?

4. What mechanism could be accounted for a distinct step-like horizontal transverse structure of the fronts repeatedly observed north of the Crozet and Kerguelen Plateaus? Does the topography influence (or induce) this phenomenon? How coherent is this structure in depth and along the fronts?

The newly created, extended data base enables us to set out the study of seasonal, interannual and decadal variability of the Southern Ocean fronts and their relation to the climate change. The data coverage, though, is strongly nonuniform, with data-sparse areas west of the Crozet Plateau and east of the Kerguelen-Amsterdam Passage. Meanwhile, these are the key regions where the fronts confluence and split again. The large-scale, detailed, multiship, synoptic CTD/SeaSoar surveys of these areas deserve the highest priority in any program of observational studies of the South Indian/Antarctic Ocean.

Acknowledgments. V.Yakovlev, B.Trotsenko, A.Klyausov, and V.Lanin supplied a vast amount of valuable data from the YugNIRO archive, processed by B.Haines, P.Mele, and A.Martino at the LDEO. A.Martino also produced innumerable maps and contoured sections, handling the ever-increasing data base. Several modern high-quality CTD data sets were kindly provided by the originators (Principal Investigators), namely, Y.-H.Park (*Marion Dufresne* cruise 68), R.Pollard (*Discovery* cruise 164), W.Roether (*Meteor* cruise 11). Y.-H.Park and L.Gambéroni sent us also data of other *Marion Dufresne* cruises. L.Hamilton supplied the most recent Australian data. The text was much improved thanks to the comments of T.Whitworth and especially Y.-H.Park. Major revisions of the manuscript were stimulated by two anonymous reviewers, to whom we extend our most sincere gratitude. The work was completed mostly at the LDEO where I.B. was a visiting scientist for 14 months in 1991-1995. This opportunity and the hospitality of LDEO are greatly appreciated. The final phase of the work was completed while I.B. held the National Research Council (NRC) Senior Research Associateship with Ocean Climate Laboratory (OCL) of the NODC(NOAA); the support by the NRC and OCL (Sydney Levitus, Director) is gratefully acknowledged. This work was supported by National Science Foundation grant OPP 90-24755 from Office of Polar Programs. LDEO contribution No. 5400.

References

Belkin, I. M., Control and editing of oceanographic data (general principles)(in Russian), *Tr. Vses. Nauchno-Issled. Inst. Gidrometeorol. Inf. Mirovogo Tsentra Dannykh, 113*, 108-113, 1984a.

Belkin, I. M. Semantic control and editing of hydrographic station data (in Russian), *Tr. Vses. Nauchno-Issled. Inst. Gidrometeorol. Inf. Mirovogo Tsentra Dannykh, 113*, 99-108, 1984b.

Belkin, I. M., Main hydrological features of the central South Pacific (in Russian), in *Ekosistemy Subantarkticheskoy Zony Tikhogo Okeana* (*Ecosystems of the Subantarctic Zone of the Pacific Ocean*), edited by M.E.Vinogradov and M.V.Flint, pp. 21-28, Nauka, Moscow, 1988a.

Belkin, I. M., Hydrological fronts of the Indian Subantarctic by data of the Japanese Antarctic Research Expeditions (JARE), 27 pp., P.P.Shirshov Inst. of Oceanol., Acad. of Sci. USSR, Moscow, 1988b. (Available as 6135-B88 from All-Union Inst. for Sci. and Tech. Inf. (VINITI), Moscow.)

Belkin, I. M., Thermohaline structure, hydrological fronts, and flux of the Antarctic Circumpolar Current in the central part of the Indian sector of the Southern Ocean (in Russian), *Antarktika, 28*, 97-112, 1989a.

Belkin, I. M., Alteration of the front distributions in the Southern Ocean near the Crozet Plateau, *Dokl. Acad. Sci. USSR, Earth Sci. Sec.*, Engl. Transl., *308*, 265-268, 1989b.

Belkin, I. M., Hydrological fronts of the Indian Subantarctic (in Russian), *Antarktika, 29*, 119-128, 1990.

Belkin, I. M., *Morphostatistical Analysis of Ocean Stratification* (in Russian), 134 pp., Gidrometeoizdat, Leningrad, 1991.

Belkin, I. M., Frontal structure of the South Atlantic (in Russian), in *Pelagicheskie Ekosistemy Yuzhnogo Okeana* (*Pelagic Ecosystems of the Southern Ocean*), edited by N.M.Voronina, pp. 40-53, Nauka, Moscow, 1993a.

Belkin, I. M., Horizontal structure of the surface thermohaline fronts of the Southern Ocean (in Russian), *Antarktika, 31*, 109-127, 1993b.

Belkin, I. M., Frontal structure of the South Atlantic (abstract), in *The South Atlantic: Present and Past Circulation, Ber. 52*, pp. 19-20, Fachber. Geowiss., Univ. of Bremen, 1994.

Belkin, I. M., and A. L. Gordon, Southern Ocean frontal structure from the Greenwich Meridian to Tasmania (abstract), *Eos Trans. AGU, 74*(16), Spring Meet. suppl., 181, 1993.

Belkin, I. M. and Yu. A. Romanov, Surface currents and thermal fronts of the South Indian Ocean, *Oceanology*, Engl. Transl., *30*, 35-39, 1990.

Belkin, I. M., V. A. Bochkov, and M. Yu. Romanov, Hydrological fronts of the Southern Ocean, Summer 1988/89 (in Russian), *Antarktika, 30*, 89-96, 1991.

Böhnecke, G., Temperatur, Salzgehalt und Dichte an der Oberfläche des Atlantischen Ozeans, *Meteor Rep., 5*, 1-249, 1936.

Botnikov, V. N., Geographical position of the Antarctic Convergence zone in the Southern Ocean (in Russian), *Sov. Antarct. Exped. Inf. Bull.*, Engl. Transl., *4*(41), 324-327, 1963.

Burling, R. W., Hydrology of circumpolar waters south of New Zealand, *N. Z. DSIR Bull., 143*, 66 pp., 1961.

Buinitsky, V. Ch., *Sea Ice and Icebergs of the Antarctic* (in Russian), 256 pp., Izd. LGU, Leningrad, 1973.

Chelton, D. B., M. G. Schlax, D. L. Witter, and J. G. Richman, Geosat altimeter observations of the surface circulation of the Southern Ocean, *J. Geophys. Res., 95*, 17,877-17,903, 1990.

Clifford, M. A., A descriptive study of the zonation of the Antarctic Circumpolar Current and its relation to wind stress and ice cover, M.S.thesis, 93 pp., Texas A&M Univ., College Station, 1983.

Cresswell, G. R., The Leeuwin Current--Observations and recent models, *J. Roy. Soc. West. Aust., 74*, 1-4, 1991.

Daniault, N., and Y. Ménard, Eddy kinetic energy distribution in the Southern Ocean from altimetry and FGGE drifting buoys, *J. Geophys. Res., 90*, 11,877-11,889, 1985.

Deacon, G. E. R., A general account of the hydrology of the South Atlantic Ocean, *Discovery Rep., 7*, 171-238, 1933.

Deacon, G. E. R., The hydrology of the Southern Ocean, *Discovery Rep., 15*, 1-124, 1937.

Deacon, G. E. R., Water circulation and surface boundaries in the oceans, *Q. J. R. Meteorol. Soc., 71*, 11-25, 1945.

Deacon, G. E. R., The southern cold temperate zone, *Proc. R. Soc., London, B, 152*, 441-447, 1960.

Deacon, G. E. R., Physical and biological zonation in the Southern Ocean, *Deep Sea Res., 29*, 1-15, 1982.

Deacon, G. E. R., Kerguelen, Antarctic and subantarctic, *Deep Sea Res., 30*, 77-81, 1983.

Delépine, R., *Les discontinuités océanographiques dans l'Ouest de l'Ocean Indien, d'après la température de l'eau de mer superficielle*, Com. Natl. Fr. Rech. Antarct., *3*, 25-61, 1963.

Deutsche Hydrographische Institut, Monatskarten für den Indischen Ozean, *Nr. 2422*, Hamburg, 1960.

Edwards, R. J., and W. J. Emery, Australasian Southern Ocean

frontal structure during summer 1976-77, *Aust. J. Mar. Freshwater Res., 33*, 3-22, 1982.
Emery, W. J., Antarctic Polar Frontal Zone from Australia to the Drake Passage, *J. Phys. Oceanogr., 7*, 811-822, 1977.
Gambéroni, L., J. Géronimi, P. F. Jeannin, and J. F. Murail, Study of frontal zones in the Crozet-Kerguelen region, *Oceanol. Acta, 5*, 289-299, 1982.
Garner, D. M., The Antarctic convergence south of New Zealand, *N. Z. J. Geol. Geophys., 1*, 577-594, 1958.
Garrett, J., Oceanographic features revealed by the FGGE drifting buoy array, in *Oceanography From Space*, edited by J.F.R.Gower, pp. 61-69, Plenum, New York, 1981.
Gordon, A. L., Structure of Antarctic waters between 20°W and 170°W, *Antarct. Map Folio Ser.*, folio 6, edited by V.C.Bushnell, 10 pp. with maps, Am. Geogr. Soc., New York, 1967.
Gordon, A. L., Antarctic Polar Front Zone, in *Antarctic Oceanology I, Antarct. Res. Ser.*, vol.15, edited by J.L.Reid, pp. 205-221, AGU, Washington, D.C., 1971.
Gordon, A. L., and K. T. Bosley, Cyclonic gyre in the tropical South Atlantic, *Deep Sea Res., 38*, suppl.1, S323-S343, 1991.
Gordon, A. L., and R. D. Goldberg, Circumpolar characteristics of Antarctic waters, in *Antarct. Map Folio Ser.*, folio 13, edited by V.Bushnell, Am. Geogr. Soc., New York, pp. 1-15, 1970.
Gordon, A. L., H. W. Taylor, and D. T. Georgi, Antarctic oceanographic zonation, in *Polar Oceans*, edited by M.J.Dunbar, pp. 45-76, Arct. Inst. of North Am., Calgary, 1977a.
Gordon, A. L., D. T. Georgi, and H. W. Taylor, Antarctic Polar Front Zone in the western Scotia Sea, *J. Phys. Oceanogr., 7*, 309-328, 1977b.
Gordon, A. L., E. Molinelli, and T. Baker, Large-scale relative dynamic topography of the Southern Ocean, *J. Geophys. Res., 83*, 3023-3032, 1978.
Gordon, A. L., E. Molinelli, and T. Baker, *The Southern Ocean Atlas*, 35 pp.+248 plates, Columbia Univ. Press, New York, 1982.
Gordon, A. L., J. R. E. Lutjeharms, and M. L. Gründlingh, Stratification and circulation at the Agulhas Retroflection, *Deep Sea Res., 34*, 565-599, 1987.
Gordon, A. L., R. F. Weiss, W. M. Smethie Jr., and M. J. Warner, Thermocline and intermediate water communication between the South Atlantic and Indian Oceans, *J. Geophys. Res., 97*, 7223-7240, 1992.
Gouretski, V. V., Surface thermal fronts in the Atlantic sector of the Southern Ocean, *Sov. Meteorol. and Hydrol.*, Engl. Transl., no. 8, 81-89, 1987.
Gouretski, V. V. and A. I. Danilov, Weddell Gyre: Structure of the eastern boundary, *Deep Sea Res., 40*, 561-582, 1993.
Gründlingh, M. L., On the course of the Agulhas Current, *S. Afr. Geogr. J., 65*, 49-57, 1983.
Halpern, D., W. Knauss, O. Brown, and F. Wentz, An atlas of monthly mean distributions of SSMI surface wind speed, Argos buoy drift, AVHRR/2 sea surface temperature, and ECMWF surface wind components during 1991. *JPL Publ. 93-10*, 111 pp., Pasadena, Calif., 1993.
Hellerman, S., and M. Rosenstein, Normal monthly wind stress over the world ocean with error estimates, *J. Phys. Oceanogr., 13*, 1093-1104, 1983.
Hofmann, E. E., The large-scale horizontal structure of the Antarctic Circumpolar Current from FGGE drifters, *J. Geophys. Res., 90*, 7087-7097, 1985.
Hoshiai, T., M. Murano, K. Nasu, and M. Terazaki, Japanese activities for BIOMASS, *Antarct. Rec., 35*, 402-433, 1991.
Houtman, T. J., Surface temperature gradients at the Antarctic convergence, *N. Z. J. Geol. Geophys., 7*, 245-270, 1964.
Johnson, M. A., Southern Ocean surface characteristics from FGGE buoys, *J. Phys. Oceanogr., 19*, 696-705, 1989.
Joyce, T. M., W. Zenk, and J. M. Toole, The anatomy of the Antarctic Polar Front in the Drake Passage, *J. Geophys. Res., 83*, 6093-6114, 1978.
Klyausov, A. V., Position of the South Polar Front near Kerguelen and Heard Islands in the autumn of 1987, *Oceanology*, Engl. Transl., *30*, 142-148, 1990.
Kostianoy, A. G., and I. M. Belkin, A survey of observations on intrathermocline eddies in the World Ocean, in *Mesoscale/Synoptic Coherent Structures in Geophysical Turbulence, Elsevier Oceanogr. Ser.*, vol.50, edited by J.C.J.Nihoul and B.M.Jamart, pp. 821-841, Elsevier, New York, 1989.
Levitus, S., *Climatological Atlas of the World Ocean, NOAA Prof. Pap. 13*, 173 pp.+17 fiche, U.S. Govt. Print. Off., Washington, D.C., 1982.
Lutjeharms, J. R. E., Location of frontal systems between Africa and Antarctica: Some preliminary results, *Deep Sea Res., 32*, 1499-1509, 1985.
Lutjeharms, J. R. E., and W. J. Emery, The detailed thermal structure of the upper ocean layers between Cape Town and Antarctica during the period Jan.-Feb. 1978, *S. Afr. J. Antarct. Res., 13*, 3-14, 1983.
Lutjeharms, J. R. E., and H. R. Valentine, Southern Ocean thermal fronts south of Africa, *Deep Sea Res., 31*, 1461-1475, 1984.
Lutjeharms, J. R. E., and R. C. Van Ballegooyen, Topographic control in the Agulhas Current system, *Deep Sea Res., 31*, 1321-1337, 1984.
Lutjeharms, J. R. E., and R. C. Van Ballegooyen, The retroflection of the Agulhas Current, *J. Phys. Oceanogr., 18*, 1570-1583, 1988.
Lutjeharms, J. R. E., H. R. Valentine, and R. C. Van Ballegooyen, On the Subtropical Convergence in the South Atlantic Ocean, *S. Afr. J. Sci., 89*, 552-559, 1993.
Mackintosh, N. A., The Antarctic convergence and distribution of surface temperature in Antarctic waters, *Discovery Rep., 23*, 177-212, 1946.
Matsumoto, K., and M. Mine, Oceanographic data of the 21st Japanese Antarctic Research Expedition from November 1979 to April 1980, *JARE Data Rep., 75*, 44 pp., 1982.
Matsuura, N., D. Inagake, J. Fukuoka, and A. Kitazawa, Oceanographic conditions of the Southern Ocean south of Australia during the summer of 1984, *Trans. Tokyo Univ. Fish., 6*, 9-22, 1985.
McCartney, M. S., Subantarctic Mode Water, in *A Voyage of Discovery, George Deacon 70th Anniversary Volume*, edited by M.Angel, 103-119, Pergamon, New York, 1977.
McCartney, M. S., The subtropical recirculation of mode waters, *J. Mar. Res., 40*, suppl., 427-464, 1982.
Meinardus, W., *Meteorologische Ergebnisse der Deutschen Südpolar Expedition 1901/03*, vol. *3*, *Meteorologie*, half I, part 3, 238 pp., Berlin, 1923.
Michida, Y., and S. Inazumi, Oceanographic data of the 28th Japanese Antarctic Research Expedition from November 1986 to April 1987, *JARE Data Report No.139*, 75 pp., 1988.
Nagata, Y., Y. Michida, and Y. Umimura, Variation of positions and structures of the oceanic fronts in the Indian Ocean sector of the Southern Ocean in the period from 1965 to 1987, in *Antarctic Ocean and Resources Variability*, edited by D.Sahrhage, pp. 92-98, Springer-Verlag, New York, 1988.
Nowlin, W. D. , Jr., and M. Clifford, The kinematic and thermohaline zonation of the Antarctic Circumpolar Current at Drake Passage, *J. Mar. Res., 40*, suppl., 481-507, 1982.
Nowlin, W. D., Jr., and J. M. Klinck, The physics of the Antarctic Circumpolar Current, *Rev. Geophys., 24*, 469-491, 1986.
Nowlin, W. D., Jr., T. Whitworth III, and R. D. Pillsbury, Structure and transport of the Antarctic Circumpolar Current at Drake Passage from short-term measurements, *J. Phys. Oceanogr., 7*, 788-802, 1977.
Olbers, D., V. Gouretski, G. Seiß, and J. Schröter, *Hydrographic Atlas of the Southern Ocean*, 17 pp.+82 plates, Alfred Wegener Inst., Bremerhaven, 1992.
Orsi, A. H., W. D. Nowlin Jr., and T. Whitworth III, On the circulation and stratification of the Weddell Gyre, *Deep Sea Res., 40*, 169-203, 1993.
Orsi, A. H., T. Whitworth III, and W. D. Nowlin Jr., On the meridional extent and fronts of the Antarctic Circumpolar Current, *Deep Sea Res., 42*, 641-673, 1995.
Ostapoff, F., The salinity distribution at 200 meters and the Antarctic frontal zones, *Dtsch. Hydrogr. Z., 15*, 133-142, 1962.
Park, Y.-H., E. Charriaud, L. Gambéroni, A. Lamy, and B. Saint-Guily, Structure et variabilité du Courant Circumpolaire Antarctique dans la région Kerguelen-Amsterdam, *C.R.Acad.Sci., 308, Ser. 2*, 177-183, 1989.
Park, Y.-H., L. Gambéroni, and E. Charriaud, Frontal structure

and transport of the Antarctic Circumpolar Current in the south Indian Ocean sector, 40-80°E, *Mar. Chem.*, *35*, 45-62, 1991.

Park, Y.-H., L. Gambéroni, and E. Charriaud, Frontal structure, water masses and circulation in the Crozet Basin, *J. Geophys. Res.*, *98*, 12,361-12,385, 1993.

Patterson, S. L., and H. A. Sievers, Mesoscale thermal structure of the Polar Frontal Zone in Drake Passage during the austral summer of 1976, *Ser. Cient. Inst. Antárt. Chil.*, *25/26*, 49-112, 1979/1980.

Patterson, S. L., and H. A. Sievers, The Weddell-Scotia Confluence, *J. Phys. Oceanogr.*, *10*, 1584-1610, 1980.

Patterson, S. L., and T. Whitworth III, Physical Oceanography, in *Antarctic Sector of the Pacific*, edited by G.P.Glasby, pp. 55-93, Elsevier, New York, 1990.

Pearce, A. F., Eastern boundary currents of the southern hemisphere, *J. R. Soc. West. Aust.*, *74*, 35-45, 1991.

Peterson, R. G., and L. Stramma, Upper-level circulation in the South Atlantic Ocean, *Prog. Oceanogr.*, *26*, 1-73, 1991.

Peterson, R. G., and T. Whitworth III, The Subantarctic and Polar Fronts in relation to deep water masses through the southwestern Atlantic, *J. Geophys. Res.*, *94*, 10,817-10,838, 1989.

Quartly, G. D., and M. A. Srokosz, Seasonal variations in the region of the Agulhas Retroflection: Studies with Geosat and FRAM, *J. Phys. Oceanogr.*, *23*, 2107-2124, 1993.

Read, J. F., and R. T. Pollard, Structure and transport of the Antarctic Circumpolar Current and Agulhas Return Current at 40°E, *J. Geophys. Res.*, *98*, 12,281-12,295, 1993.

Reid, J. L., On the total geostrophic circulation of the South Atlantic Ocean: Flow patterns, tracers, and transports, *Prog. Oceanogr.*, *23*, 149-244, 1989.

Sandwell, D. T., and B. Zhang, Global mesoscale variability from the Geosat Exact Repeat Mission: Correlation with ocean depth, *J. Geophys. Res.*, *94*, 17,971-17,984, 1989.

Scientific Committee on Oceanic Research (SCOR) Working Group 74, General circulation of the Southern Ocean: Status and recommendations for research, *Rep. WCP-108*, 54 pp., World Clim. Programme, World Meteorol. Organ., Geneva, 1985.

Shannon, L. V., D. E. Pollock, P. Chapman, and A. A. Robertson, South-east Atlantic Expedition of R.S. *Africana*, April 1989: Some preliminary results, *S. Afr. J. Sci.*, *85*, 665-669, 1989.

Sievers, H. A., and W. J. Emery, Variability of the Antarctic Polar Frontal Zone in Drake Passage -- Summer 1976-1977, *J. Geophys. Res.*, *83*, 3010-3022, 1978.

Sievers, H. A., and W. D. Nowlin, Jr., The stratification and water masses at Drake Passage, *J. Geophys. Res.*, *89*, 10,489-10,514, 1984.

Sparrow, M. D., K. J. Heywood, J. Brown, and D. P. Stevens, Current structure of the South Indian Ocean, *J. Geophys. Res.*, in press, 1995.

Stramma, L., The South Indian Ocean Current, *J. Phys. Oceanogr.*, *22*, 421-430, 1992.

Stramma, L., and R. G. Peterson, The South Atlantic Current, *J. Phys. Oceanogr.*, *20*, 846-859, 1990.

Sverdrup, H. U., M. Johnson, and R. Fleming, *The Oceans, Their Physics, Chemistry and General Biology*, 1887 pp., Prentice Hall, Englewood Cliffs, N.J., 1942.

Taylor, H., A. L. Gordon, and E. Molinelli, Climatic characteristics of the Antarctic polar front zone, *J. Geophys. Res.*, *83*, 4572-4578, 1978.

Tsuchiya, M., L. D. Talley, and M. S. McCartney, Water mass distributions in the western South Atlantic: A section from South Georgia Island (54S) northward across the equator, *J. Mar. Res.*, *52*, 55-81, 1994.

Valentine, H. R., J. R. E. Lutjeharms, and G. B. Brundrit, The water masses and volumetry of the southern Agulhas Current region, *Deep Sea Res.*, *40*, 1285-1305, 1993.

Vinogradov, M. E., and M. V. Flint, Study of the pelagic ecosystems of the subantarctic waters of the Pacific Ocean (34th cruise of the R/V *Dmitriy Mendeleyev*, December 16, 1984 - April 15, 1985), *Oceanology*, Engl. Transl., *26*, 541-543, 1986.

Webb, D. J., P. D. Killworth, A. C. Coward, and S. R. Thompson, *The FRAM Atlas of the Southern Ocean*, 67 pp., Nat. Environ. Res. Counc., Swindon, 1991.

Whitworth, T., III, Zonation and geostrophic flow of the Antarctic Circumpolar Current at Drake Passage, *Deep Sea Res.*, 27, 497-507, 1980.

Whitworth, T., III, and W. D. Nowlin Jr., Water masses and currents of the Southern Ocean at the Greenwich meridian, *J. Geophys. Res.*, 92, 6462-6476, 1987.

Zillman, J. W., Sea surface temperature gradients south of Australia, *Aust. Meteorol. Mag.*, 18, 22-30, 1970.

I. M. Belkin, Ocean Climate Laboratory, National Oceanographic Data Center, NOAA, E/OC5, 1315 East-West Highway, Silver Spring, MD 20910-3282. (e-mail: ibelkin@nodc.noaa.gov)

A. L. Gordon, Lamont-Doherty Earth Observatory, Columbia University, Palisades, NY 10964.

(Received November 19, 1993; revised May 17, 1995; accepted June 27, 1995.)